

# Bootstrapping Quantum Particles and their Bounds

Takeshi MORITA<sup>a,b\*</sup>

*a. Department of Physics, Shizuoka University  
836 Ohya, Suruga-ku, Shizuoka 422-8529, Japan*

*b. Graduate School of Science and Technology, Shizuoka University  
836 Ohya, Suruga-ku, Shizuoka 422-8529, Japan*

## Abstract

The range of motion of a particle with certain energy  $E$  confined in a potential is determined from the energy conservation law in classical mechanics. The counterpart of this question in quantum mechanics can be thought of as what the possible range of the expectation values of the position operator  $\langle x \rangle$  of a particle, which satisfies  $E = \langle H \rangle$ . This range would change depending on the state of the particle, but the universal upper and lower bounds, which is independent of the state, must exist. In this study, we show that these bounds can be derived by using the bootstrap method. We also point out that the bootstrap method can be regarded as a generalization of the uncertainty relations, and it means that the bounds are determined by the uncertainty relations in a broad sense. Furthermore, the bounds on possible expectation values of various quantities other than position can be determined in the same way. However, in the case of multiple identical particles (bosons and fermions), we find some difficulty in the bootstrap method. Because of this issue, the predictive power of the bootstrap method in multi-particle systems is limited in the derivation of observables including energy eigenstates. In addition, we argue an application of the bootstrap method to thermal equilibrium states. We find serious issues that temperature and entropy cannot be handled. Although we have these issues, we can derive some quantities in microcanonical ensembles of integrable systems governed by generalized Gibbs ensembles.

---

\*E-mail address: morita.takeshi(at)shizuoka.ac.jp

# Contents

<b>1</b>	<b>Introduction</b>	<b>2</b>
<b>2</b>	<b>Bootstrapping One-Dimensional Particle</b>	<b>3</b>
2.1	Bounds on expectation values in quantum mechanics . . . . .	3
2.2	Bootstrap analysis . . . . .	6
2.2.1	Bootstrap analysis and the uncertainty relations . . . . .	7
2.3	Bootstrapping general states with $E = \langle H \rangle$ . . . . .	8
2.3.1	Examples: Anharmonic oscillator and double-well potential . . . . .	8
2.4	Bootstrapping stationary states with $E = \langle H \rangle$ . . . . .	10
2.4.1	Example: Anharmonic oscillator . . . . .	11
2.5	Bootstrapping energy eigenstates . . . . .	13
2.5.1	Example: Anharmonic oscillator . . . . .	13
2.6	Summary of the one-dimensional problem . . . . .	14
<b>3</b>	<b>Bootstrapping Two-Particle Systems</b>	<b>15</b>
3.1	Problems in identical particles . . . . .	15
3.1.1	Example 1: Non-interacting harmonic oscillators . . . . .	16
3.1.2	Example 2: Yang-Mills quantum mechanics . . . . .	17
3.1.3	Bootstrapping other states with $E = \langle H \rangle$ in YMQM . . . . .	20
<b>4</b>	<b>Bootstrapping Thermal Equilibrium States</b>	<b>22</b>
4.1	Difficulties in bootstrapping canonical ensemble . . . . .	23
4.2	Bootstrapping micro-canonical ensemble . . . . .	24
4.3	Bootstrapping free particles in micro-canonical ensembles . . . . .	25
4.3.1	Example 1: Non-interacting $N$ harmonic oscillators . . . . .	25
4.3.2	Example 2: Non-interacting $N$ anharmonic oscillator . . . . .	26
4.3.3	Thermometer? . . . . .	28
<b>5</b>	<b>Discussions</b>	<b>29</b>
<b>A</b>	<b>Analytic Results on the Bounds</b>	<b>30</b>
A.1	States saturating the bound (2.4) . . . . .	31
A.2	States saturating the bound (2.5) . . . . .	31
A.3	Bounds on $\langle p \rangle$ in general $V(x)$ . . . . .	31

## 1 Introduction

In classical mechanics, it is a simple problem to find the range of motion of a particle confined in a potential. For simplicity, we consider an one-dimensional non-relativistic particle with the mass 1 in a potential  $V(x)$ . If the particle has energy  $E$ , the turning points  $x_1$  and  $x_2$  ( $x_1 < x_2$ ) that satisfy  $E = V(x_i)$  ( $i = 1, 2$ ) would be determined through the energy conservation law

$$E = \frac{1}{2}p^2 + V(x), \quad (1.1)$$

and the range is given by  $x_1 \leq x \leq x_2$ .

What is the answer to this question in quantum mechanics? One answer is that the particle can pass through the potential in quantum mechanics, and therefore the possible range of the position  $x$  of the particle is  $-\infty \leq x \leq \infty$ . However, this answer is not practical because the probability of taking such a large range would be very small. So, the counterpart of this problem in quantum mechanics may be “If a particle satisfies  $E = \langle H \rangle$ , what is the possible range of the expectation value of the particle’s position operator  $x$ ?” This range would depends not only on the energy but also on the state of the particle. However, there must be some universal upper and lower bounds that are independent of the state. In this paper, we study these bounds. Similar questions can be asked for the expectation values of various observables. If the system has a certain energy, how are the maximum and minimum bounds of these expectation values determined?

The flavor of this problem may be similar to that of the uncertainty relations. The uncertainty relations are that there are some universal restrictions between observables (especially variances). In the case of the above problem, we seek the restrictions of observables under the single constraint that the system has energy  $E$ . Thus, the uncertainty relation might play some role.

Actually, we can easily show that the problem in harmonic oscillators can be solved by using the uncertainty relation. However, this method cannot be applied to more general potential cases. There, we may need some generalization of the uncertainty relations. In this paper, we point out that the bootstrap method studied by Han et al [1], which was originally proposed as a new method to derive the spectrum of the energy eigenstates in quantum mechanics, can be regarded as a generalization of the uncertainty relations. Then, by using the bootstrap method, we will numerically find the bounds in general potential cases. Therefore, the problem is indeed closely related to the uncertainty relations. (It means that the original bootstrap method [1] may also be

interpreted as a derivation of the spectrum of the energy eigenstates by applying the uncertainty relations.)

This problem can be asked to multi-particle systems too. However, we find that the bootstrap method has difficulty in handling the statistical nature of identical particles (bosons and fermions) and it can provide only a limited answer. Related to this issue, the predictive power of the numerical bootstrap method for the energy eigenstates is also limited, if identical particles are involved.

We also consider an application of the bootstrap method to thermal equilibrium states in multi-particle systems. However, due to the issue of the identical particles, the bootstrap method can provide only limited predictions. (As we will see, this issue might be evaded in quantum field theories and lattice systems.) In addition, we also find a serious issue that the bootstrap method cannot handle temperature and entropy. On the other hand, we will show that, as an exception, the method can predict physical quantities in a microcanonical ensemble when the system is integrable and the thermal equilibrium state obeys a generalized Gibbs ensemble [2]. Therefore, the bootstrap method may not be useless for thermal equilibrium states of multi particles.

The organization of this paper is as follows. In section 2, we study the problem of finding the bounds on the expectation values of observables under the constraint  $E = \langle H \rangle$  in one-dimensional quantum mechanics. We show that this problem can be solved by using the uncertainty relation in harmonic oscillators. For more complicated cases, we can use the numerical bootstrap method to solve the problem. We also show that the bootstrap method can be regarded as a generalization of the uncertainty relations. In section 3, two-particle systems is considered. There, we will see that the bootstrap method has an issue on identical particles (bosons and fermions), and its predictive power is limited. In section 4, we show our attempt to apply the bootstrap method to thermal equilibrium states in multi-particle systems. We will see that the bootstrap method has a serious issue that temperature and entropy cannot be handled. But it may work in integrable systems. Section 5 contains conclusions and discussions.

## 2 Bootstraping One-Dimensional Particle

### 2.1 Bounds on expectation values in quantum mechanics

We study how the upper and lower bounds on the expectation value  $\langle Q \rangle$  of a physical observable  $Q$  are determined in quantum mechanics when the system satisfies  $E = \langle H \rangle$ . We start from an

one-dimensional quantum mechanics,

$$H = \frac{1}{2}p^2 + V(x). \quad (2.1)$$

We assume  $V(x) \rightarrow +\infty$ , ( $x \rightarrow \pm\infty$ ). Our goal is to find the maximum (minimum) value of  $\langle Q \rangle$  among all possible mixed states that satisfy the constraint  $E = \langle H \rangle$ . Even if all the energy eigenstates of this system are known, this is a non-trivial question<sup>1</sup>.

The flavor of this problem is similar to that of the uncertainty relations, and it is natural to employ them to find the bounds on  $\langle Q \rangle$ . In fact, this attempt works for harmonic oscillators. Let us consider the following model,

$$H = \frac{1}{2}p^2 + \frac{1}{2}x^2. \quad (2.2)$$

First, we take  $Q = x$  and investigate its bounds. Through the constraint  $E = \langle H \rangle$ , we obtain

$$\begin{aligned} E &= \frac{1}{2}\langle p^2 \rangle + \frac{1}{2}\langle x^2 \rangle = \frac{1}{2}(\langle \Delta p^2 \rangle + \langle p \rangle^2) + \frac{1}{2}(\langle \Delta x^2 \rangle + \langle x \rangle^2) \\ &\implies \langle x \rangle^2 + \langle p \rangle^2 = 2E - (\langle \Delta x^2 \rangle + \langle \Delta p^2 \rangle) \geq 2E - 2\sqrt{\langle \Delta x^2 \rangle \langle \Delta p^2 \rangle} \geq 2E - \hbar. \end{aligned} \quad (2.3)$$

Here,  $\langle \Delta O^2 \rangle := \langle O^2 \rangle - \langle O \rangle^2$  denotes the deviation of  $O$ . We used the arithmetic and geometric means in the first inequality, and used the uncertainty relation  $\Delta x^2 \Delta p^2 \geq \hbar^2/4$  in the second inequality. From this equation, the bounds are derived,

$$-x_*(E) \leq \langle x \rangle \leq x_*(E), \quad x_*(E) := \sqrt{2(E - \hbar/2)}. \quad (2.4)$$

We compare this result with the classical mechanics. In the classical mechanics, the possible range of  $x$  is given by  $|x| \leq \sqrt{2E}$ . Thus, if we replace  $E \rightarrow E - \hbar/2$  in this relation, the quantum bounds (2.4) are reproduced. Since  $\hbar/2$  is the zero-point energy of the harmonic oscillator, this result implies that the range of  $\langle x \rangle$  in quantum mechanics is narrowed by the zero-point energy. As  $E$  increases, the difference between quantum mechanics and classical mechanics becomes relatively small, and it explains why  $|x| \leq \sqrt{2E}$  works in the classical limit. These are illustrated in Fig. 1.

Similarly, we can derive the bounds on  $Q = x^2$  through the uncertainty relation,

$$\begin{aligned} 2E &= 2\langle H \rangle = \langle p^2 \rangle + \langle x^2 \rangle \geq \langle x^2 \rangle + \frac{\hbar^2}{4\langle x^2 \rangle} \\ &\implies E - \sqrt{E^2 - \hbar^2/4} \leq \langle x^2 \rangle \leq E + \sqrt{E^2 - \hbar^2/4}. \end{aligned} \quad (2.5)$$

---

<sup>1</sup>Even if we restrict the state to pure states, this problem is still non-trivial. In this case, a pure state is given by  $\sum b_n |n\rangle$ , where  $|n\rangle$  is the energy eigenstate and  $b_n$  is a complex number. Then, our task is finding a set of parameter  $\{b_n\}$  such that  $\langle Q \rangle$  is maximized (minimized) under the constraint  $\langle H \rangle = E$ . This is a non-linear optimization problem with respect to  $\{b_n\}$ , which is difficult to solve in general.

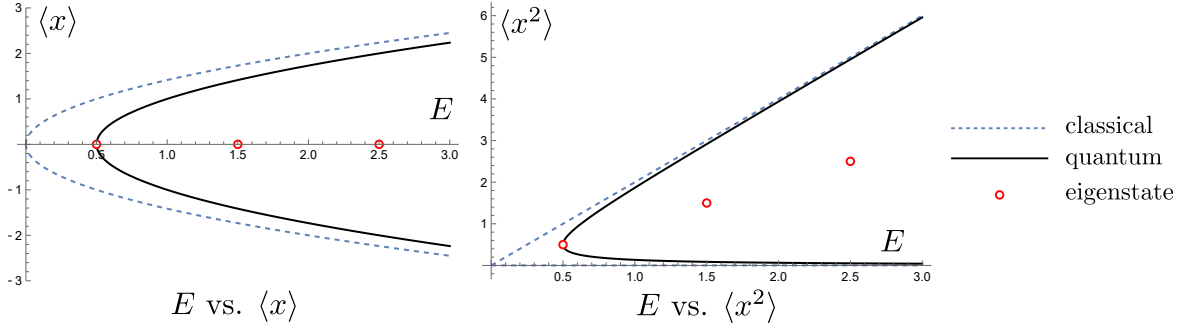


Figure 1: The bounds on  $\langle x \rangle$  and  $\langle x^2 \rangle$  in the harmonic oscillator (2.2). The regions enclosed by the dashed lines are the predictions from classical mechanics, and those enclosed by the solid lines are those from quantum mechanics derived in (2.4) and (2.5). The red circles are the energy eigenstates. The regions in quantum mechanics are narrower than classical mechanics because of the restriction through the uncertainty relation. In these plots, we have taken  $\hbar = 1$ .

In classical mechanics, the range of the possible value of  $\langle x^2 \rangle = \langle x \rangle^2 = x^2$  is given by  $0 \leq x^2 \leq 2E$ . Thus, the result in quantum mechanics (2.5) is again narrower than the classical one. It can be regarded as a consequence of the uncertainty relation, which restricts the range of physical quantities more than classical mechanics.

So far, we have investigated the upper and lower bounds on  $\langle x \rangle$  and  $\langle x^2 \rangle$ . Similarly, we can also obtain the bounds on  $\langle p \rangle$  and  $\langle p^2 \rangle$ . However, we have not shown whether states saturating these inequalities really exist or not. If not, stronger bounds must exist. In fact, from a simple consideration, we can show that certain coherent states saturate the bounds on  $\langle x \rangle$  and  $\langle p \rangle$  and that certain Gaussian wave packets saturate the bounds on  $\langle x^2 \rangle$  and  $\langle p^2 \rangle$ . Hence, (2.4) and (2.5) are the genuine bounds. The details are provided in Appendix A.1 and A.2. In addition, from similar considerations, we can derive the upper and lower bounds on  $\langle p \rangle$  in general potentials  $V(x)$  in (2.1). The details are discussed in Appendix A.3.

In this subsection, we have studied the bounds on the operators  $x$ ,  $x^2$ ,  $p$  and  $p^2$  in the harmonic oscillator (2.2). These bounds are restricted by the uncertainty relation. This is in contrast to classical mechanics, where the range of physical quantities is determined only through the energy conservation law. However, if we consider more complicated operators such as  $Q = x^4$  or general potential  $V(x)$  in (2.1), it seems to be difficult to obtain the bounds on  $\langle Q \rangle$  from simple uncertainty relations.

## 2.2 Bootstrap analysis

To find the bounds in more general situations, we apply the numerical bootstrap method proposed by Han et al [1]. As we discuss soon, this method can be regarded as a generalization of the uncertainty relations.

For this purpose, we follow Han et al and introduce a bootstrap matrix. We assume that any (non-singular) operators  $O$  in the system satisfy the following positivity condition for any (non-singular) mixed states

$$\langle O^\dagger O \rangle_\rho := \text{Tr}(\hat{\rho} O^\dagger O) \geq 0. \quad (2.6)$$

Here  $\hat{\rho}$  is defined by

$$\hat{\rho} := \sum_\alpha c_\alpha |\alpha\rangle\langle\alpha|, \quad (2.7)$$

where  $|\alpha\rangle$  are pure states that are normalized as  $\langle\alpha|\alpha\rangle = 1$ , and  $c_\alpha$  are real constants that specify the mixed state and satisfy  $0 \leq c_\alpha \leq 1$  and  $\sum_\alpha c_\alpha = 1$ . We also assume that  $O$  satisfies,

$$\langle O^\dagger \rangle_\rho = \langle O \rangle_\rho^*. \quad (2.8)$$

Then, we prepare a set of some  $K$  operators  $\{O_n\}$  and  $K$  auxiliary constants  $\{b_n\}$  ( $n = 1, \dots, K$ ), and define an operator  $\tilde{O}$ ,

$$\tilde{O} := \sum_{n=1}^K b_n O_n. \quad (2.9)$$

Now, because of the positivity (2.6),

$$\langle \tilde{O}^\dagger \tilde{O} \rangle_\rho = \sum_{m,n=1}^K b_m^* b_n \langle O_m^\dagger O_n \rangle_\rho \geq 0 \quad (2.10)$$

is satisfied for arbitrary constants  $\{b_n\}$ . Hence, the following  $K \times K$  Hermite matrix  $\mathcal{M}$  has to be positive-semidefinite [1],

$$\mathcal{M} := \begin{pmatrix} \langle O_1^\dagger O_1 \rangle_\rho & \langle O_1^\dagger O_2 \rangle_\rho & \cdots & \langle O_1^\dagger O_K \rangle_\rho \\ \langle O_2^\dagger O_1 \rangle_\rho & \langle O_2^\dagger O_2 \rangle_\rho & \cdots & \langle O_2^\dagger O_K \rangle_\rho \\ \vdots & \vdots & \ddots & \vdots \\ \langle O_K^\dagger O_1 \rangle_\rho & \langle O_K^\dagger O_2 \rangle_\rho & \cdots & \langle O_K^\dagger O_K \rangle_\rho \end{pmatrix} \succeq 0, \quad (2.11)$$

where  $\succeq$  is the mathematical symbol for a positive-semidefinite matrix. We call  $\mathcal{M}$  as a bootstrap matrix and  $\tilde{O}$  as its seed operator. We will later see that  $K$  may be regarded as a cut off parameter of numerical bootstrap analysis.

The discussion up to this point is not limited to one-dimensional quantum mechanics and it can be applied to general systems. From now on, we focus on one-dimensional quantum mechanics with the Hamiltonian (2.1). Here we take the seed operator

$$\tilde{O} = \sum_{m=0}^{K_x} \sum_{n=0}^{K_p} b_{mn} x^m p^n, \quad (2.12)$$

and construct the bootstrap matrix from it,

$$\mathcal{M} = \begin{pmatrix} 1 & \langle x \rangle_\rho & \langle p \rangle_\rho & \cdots \\ \langle x \rangle_\rho & \langle x^2 \rangle_\rho & \langle xp \rangle_\rho & \cdots \\ \langle p \rangle_\rho & \langle px \rangle_\rho & \langle p^2 \rangle_\rho & \cdots \\ \vdots & \vdots & \vdots & \ddots \end{pmatrix}. \quad (2.13)$$

The components of this matrix take the forms  $\langle p^l x^m p^k \rangle_\rho$ , but they can be described by the ordered forms  $\langle x^m p^n \rangle_\rho$  through the relation that can be derived from the commutator relation  $[x, p] = i\hbar$ ,

$$p^n x^m = \sum_{k=0}^{\min(m,n)} (-i\hbar)^k \frac{n!m!}{k!(n-k)!(m-k)!} x^{m-k} p^{n-k}. \quad (2.14)$$

In addition, these components  $\langle x^m p^n \rangle_\rho$  are restricted from the condition (2.8). For example,  $\langle px \rangle_\rho = \langle xp \rangle_\rho^* = \langle xp \rangle_\rho - i\hbar$ , and it implies that  $\text{Im}(\langle xp \rangle_\rho) = \hbar/2$ .

### 2.2.1 Bootstrap analysis and the uncertainty relations

The condition  $\mathcal{M} \succeq 0$  strongly constrains the possible values of the observables  $\langle x^m p^n \rangle_\rho$ . Actually, the uncertainty relation  $(\Delta x)^2 (\Delta p)^2 \geq \hbar^2/4$  is one of the consequences of this condition. Thus, the condition  $\mathcal{M} \succeq 0$  may be regarded as a generalized version of the uncertainty relations.

To see the derivation of the uncertainty relation from  $\mathcal{M} \succeq 0$ , we take  $K_x = K_p = 1$  in (2.9)<sup>2</sup>

$$\tilde{O} = b_{00} 1 + b_{10} x + b_{01} p. \quad (2.15)$$

Then the bootstrap matrix becomes

$$\mathcal{M} = \begin{pmatrix} 1 & \langle x \rangle & \langle p \rangle \\ \langle x \rangle & \langle x^2 \rangle & \langle xp \rangle \\ \langle p \rangle & \langle px \rangle & \langle p^2 \rangle \end{pmatrix}. \quad (2.16)$$

Here we have omitted the symbol  $\rho$ . For this matrix to be positive-semidefinite, the determinant must be non-negative, and we obtain [4],

$$\begin{aligned} (\langle x^2 \rangle - \langle x \rangle^2)(\langle p^2 \rangle - \langle p \rangle^2) &\geq |\langle xp \rangle - \langle x \rangle \langle p \rangle|^2 = \frac{1}{4} |\langle [x, p] \rangle + \langle \{x, p\} \rangle - 2 \langle x \rangle \langle p \rangle|^2 \\ &= \frac{1}{4} |\langle [x, p] \rangle|^2 + \frac{1}{4} |\langle \{x, p\} \rangle - 2 \langle x \rangle \langle p \rangle|^2 \geq \frac{1}{4} |\langle [x, p] \rangle|^2. \end{aligned} \quad (2.17)$$

---

<sup>2</sup>See [3] for a related derivation of the uncertainty relation.

Here, we have used that  $\{x, p\}$  is hermitian and  $[x, p]$  is anti-hermitian in the third equality. Then, by using  $[x, p] = i\hbar$ , we obtain the uncertainty relation

$$\Delta x^2 \Delta p^2 \geq \frac{1}{4} \hbar^2. \quad (2.18)$$

Therefore, the condition  $\mathcal{M} \succeq 0$  for a general bootstrap matrix (2.11) may be regarded as an extended version of the uncertainty relations.

### 2.3 Bootstrapping general states with $E = \langle H \rangle$

Han et al used the condition  $\mathcal{M} \succeq 0$  to obtain the spectrum of the energy eigenstates, which will be reviewed in Sec. 2.5. Here, we apply this condition to solve our problem of finding the upper and lower bounds on the expectation values of an operator  $Q$  when the system with the Hamiltonian (2.1) satisfies  $E = \langle H \rangle$ . In mathematics, this optimization problem is represented by the following symbols:

$$\begin{aligned} \max\{\langle Q \rangle_\rho \mid \mathcal{M} \succeq 0 \wedge E = \langle H \rangle_\rho = \frac{1}{2} \langle p^2 \rangle_\rho + \langle V(x) \rangle_\rho\}, \\ \min\{\langle Q \rangle_\rho \mid \mathcal{M} \succeq 0 \wedge E = \langle H \rangle_\rho = \frac{1}{2} \langle p^2 \rangle_\rho + \langle V(x) \rangle_\rho\}. \end{aligned} \quad (2.19)$$

These problems can be solved numerically using linear programming with respect to the quantities  $\{\langle x^m p^n \rangle_\rho\}$ .

#### 2.3.1 Examples: Anharmonic oscillator and double-well potential

As examples, we investigate this problem in an anharmonic oscillator and a double-well potential,

$$H = \frac{1}{2} p^2 + \frac{1}{2} x^2 + \frac{1}{4} x^4, \quad (2.20)$$

$$H = \frac{1}{2} p^2 - 5x^2 + \frac{1}{4} x^4. \quad (2.21)$$

We take  $Q = x$  and  $Q = x^2$ , and numerically compute the maximum and minimum values of the expectation values of these operators by solving the linear programming (2.19)<sup>3</sup>. The results are shown in Fig. 2 and Fig. 3. We can see that the numerical results converge as we take larger values of  $K_x$  and  $K_p$  defined in (2.12). The convergence is very quick for  $\langle x \rangle$ , and is good enough even at  $K_x = K_p = 2$ . It also seems to converge reasonably quickly for  $\langle x^2 \rangle$ . These results indicate that the numerical bootstrap method is quite effective in our problem. Here, one remark is that, similar to the uncertainty relation in the harmonic oscillator, the bootstrap method cannot tell us whether the states saturating the bounds exist or not.

---

<sup>3</sup>For these analyses, we used the Mathematica package “SemidefiniteOptimization”. We use the version 13.0 and 13.1. Note that the numerical results highly depend on the option “Method” of this package. The results presented

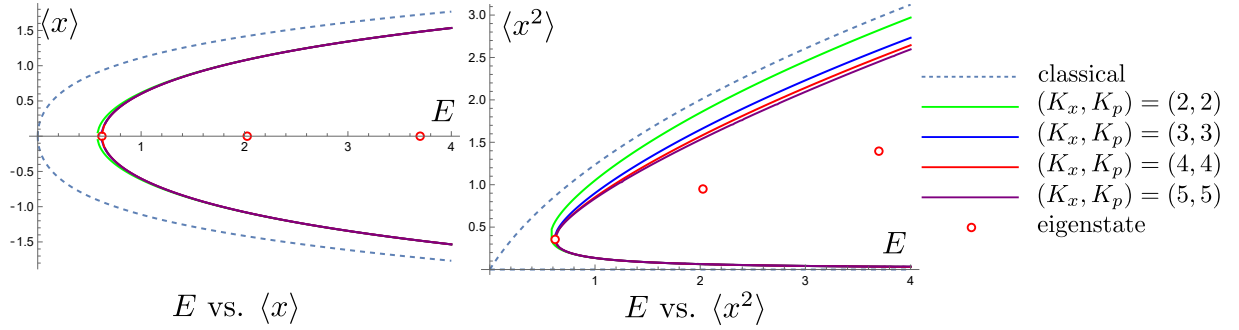


Figure 2: The ranges of the possible expectation values of  $\langle x \rangle$  and  $\langle x^2 \rangle$  in the anharmonic oscillator (2.20). The expectation values can be taken in the region enclosed by the colored solid curves in the figures. The dashed lines are for classical mechanics, and the red circles are the quantities of the energy eigenstates. As in the case of the harmonic oscillator, the ranges in quantum mechanics are narrower than those in classical mechanics. It can also be seen that the smallest possible value of  $E$  coincides with the ground state.

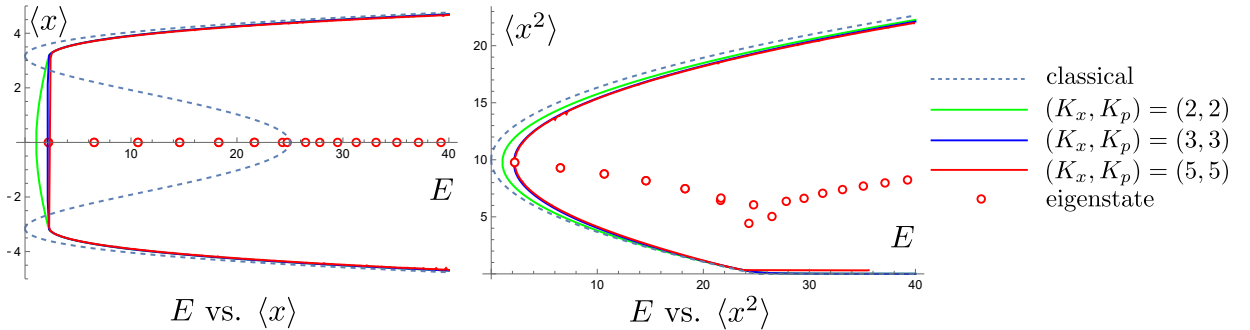


Figure 3: The range of the possible expectation values of  $\langle x \rangle$  and  $\langle x^2 \rangle$  in the double-well potential (2.21). The expectation values can be taken in the region enclosed by the colored solid curves in the figures. The dashed lines are for classical mechanics, and the red circles are for the quantities of the energy eigenstates. It can be seen that, in quantum mechanics, the range of the possible expectation values of  $\langle x \rangle$  also appears in the region not allowed in classical mechanics.

In the case of the anharmonic oscillator, the obtained results are qualitatively similar to the harmonic oscillator case shown in Fig. 1. In the case of the double-well potential,  $\langle x \rangle$  can take a value in the forbidden region in the classical mechanics<sup>4</sup>. This is expected in quantum mechanics, and our result reproduces this property.

In these numerical results, the lowest energy points coincide with the ground states<sup>5</sup>. This is because the ground state is realized as the lowest energy state among all possible states. If one simply want to find the energy of the ground state, one can obtain it by numerically solving the linear programming:  $\min\{\langle H \rangle \mid \mathcal{M} \succeq 0\}$  [7]. It implies that the ground state is the optimized state that minimizes energy under the extended version of the uncertainty relation  $\mathcal{M} \succeq 0$ , and it might give us a new picture of the ground state in quantum mechanics.

We have seen that the numerical bootstrap method works effectively in our problem. In principle, we can apply our analysis to arbitrary operators  $Q$ . However, the problem of finding the bounds on the possible values of the product of expectation values  $\langle Q_1 \rangle \langle Q_2 \rangle$  would be a nonlinear optimization problem, and it would be numerically much harder.

## 2.4 Bootstrapping stationary states with $E = \langle H \rangle$

We have seen that, when the system has energy  $E$ , the upper and lower bounds on the expectation value  $\langle Q \rangle$  can be obtained by using the bootstrap method. There, we have imposed no restrictions other than energy  $E = \langle H \rangle$  on the states. From now on, we consider the possible range of the expectation value  $\langle Q \rangle$  under an additional condition that the states are stationary. This will be a hint when we apply the bootstrap method to thermal equilibrium states, which we will discuss in Sec. 4. The general stationary state in quantum mechanics is given by the following mixed state  $\hat{\rho}_{\text{st}}$ ,

$$\hat{\rho}_{\text{st}} = \sum_{n=0}^{\infty} c_n |n\rangle \langle n|, \quad (2.22)$$

---

in Fig. 2 and Fig. 3 are obtained using Method → “DSDP”. In the numerical analysis throughout this paper,  $\hbar = 1$  is taken.

<sup>4</sup>Even in classical mechanics, if we allow probabilistic states of a particle,  $\langle x \rangle$  can take a value in the forbidden region. We do not consider such states here. A related study of the bootstrap method for classical particles was done [5, 6].

<sup>5</sup>We compute the eigenstates by numerically solving the Schrödinger equations. We use the Mathematica package “NDEigensystem” throughout this paper.

where  $|n\rangle$  ( $n = 0, 1, \dots$ ) is the energy eigenstate with the eigen energy  $E_n$ , and  $c_n$  is a constant satisfying  $0 \leq c_n \leq 1$  and  $\sum_n c_n = 1$ . Then, this state satisfies<sup>6</sup>

$$\langle [H, O] \rangle_{\rho_{\text{st}}} = 0 \quad (2.23)$$

for any operator  $O$ . Thus, in order to obtain the bounds on  $\langle Q \rangle_{\rho_{\text{st}}}$  for the stationary states with energy  $E = \langle H \rangle$ , we should add this condition to the constraints (2.19), and solve the optimization problem of finding the maximum and minimum values of  $\langle Q \rangle_{\rho_{\text{st}}}$ ,

$$\mathcal{M} \succeq 0, \quad E = \langle H \rangle_{\rho_{\text{st}}} = \frac{1}{2} \langle p^2 \rangle_{\rho_{\text{st}}} + \langle V(x) \rangle_{\rho_{\text{st}}}, \quad \langle [H, O] \rangle_{\rho_{\text{st}}} = 0, \quad (O \in \{x^m p^n\}). \quad (2.24)$$

This is again a linear programming program with respect to  $\{\langle x^m p^n \rangle_{\rho_{\text{st}}}\}$ , and we can compute it numerically.

Note that, different from the problem (2.19) discussed in Sec.2.2, we can solve this problem if we know all the energy eigenstates of the Hamiltonian. For example, if all  $\{c_n\}$  except  $c_0$  and  $c_1$  in (2.22) are zero, the range of the possible values of  $\langle Q \rangle_{\rho_{\text{st}}}$  is limited to the straight line connecting the point  $(E, \langle Q \rangle)$  at  $|0\rangle$  and  $|1\rangle$ , since  $c_0 + c_1 = 1$ . Extending it to non-zero  $\{c_n\}$ , we will obtain the region enclosed by the polygonal line connecting the eigenstates, and  $\langle Q \rangle_{\rho_{\text{st}}}$  can take a value only in this region.

#### 2.4.1 Example: Anharmonic oscillator

As an example, we seek the bounds on  $Q = x^2$  in the anharmonic oscillator (2.20). We derive the energy eigenstates by numerically solving the Schrödinger equation. The energy and  $\langle x^2 \rangle$  for each eigenstate is plotted by the red circles in Fig. 4. Then, the range of the possible values of  $\langle x^2 \rangle_{\rho_{\text{st}}}$  for the stationary states (2.22) is given by the polygonal region connecting them, which is illustrated by the dashed lines in Fig. 4. Since the constraints (2.24) are more stronger than (2.19), the range of the possible values of  $\langle x^2 \rangle$  is narrower than the range shown in Fig. 2.

We solve the same problem by computing (2.24) via the numerical bootstrap method<sup>7</sup>. The results are shown in Fig. 4<sup>8</sup>. We see that the predictions of the bootstrap method asymptotically

---

<sup>6</sup>It was pointed out in [6] that we need to take a special care on this condition when the system is on a half line such as a radial coordinate  $r \in [0, +\infty]$ .

<sup>7</sup>In this numerical problem, one question is what operator  $x^m p^n$  should be taken in the constraint  $\langle [H, O] \rangle_{\rho_{\text{st}}} = 0$  in (2.24). If more operators of  $O = x^m p^n$  are taken, the constraints become stronger, but they require greater computational resources. Here, we simply take the operators appearing in the bootstrap matrix  $\mathcal{M}$ . (Note that new operators  $O'$ , which do not exist in the bootstrap matrix  $\mathcal{M}$ , will appear from the equation  $\langle [H, O'] \rangle_{\rho_{\text{st}}} = 0$ , and we can derive new constraints  $\langle [H, O'] \rangle_{\rho_{\text{st}}} = 0$  with respect to these new operators, but we do not do it.) Similar questions arise in other bootstrap problems too and we take the same prescription throughout this paper. An exception is the energy eigenstate problem in one-dimension quantum mechanics discussed in Sec. 2.5. There, we can explicitly solve the constraints  $\langle [H, O] \rangle = 0$  and  $\langle HO \rangle = E \langle O \rangle$  [8].

<sup>8</sup>We used the Mathematica package "SemidefiniteOptimization" and take "CSDP" or "MOSEK" as the option "Method".

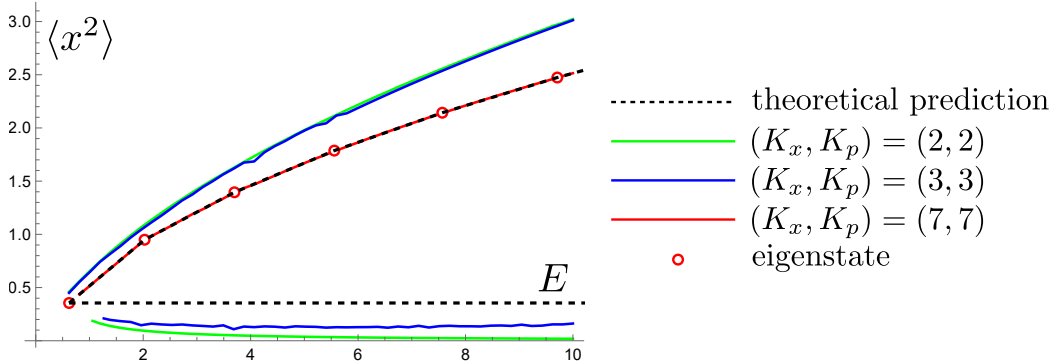


Figure 4: The range of possible values of  $\langle x^2 \rangle_{\rho_{\text{st}}}$  of the anharmonic oscillator (2.20) for stationary states (2.22). The results of the bootstrap method (2.24) converge to the theoretical predictions (the dashed lines) as  $K_x$  and  $K_p$  increase. However, the calculation of the lower bound on  $\langle x^2 \rangle_{\rho_{\text{st}}}$  is numerically difficult and does not give reliable answers. (The lower bound at  $(K_x, K_p) = (7, 7)$  is not shown in the figure, since we could not obtain reliable results.) On the other hand, the upper bound in  $E < 10$  converges well, and the results are almost identical with the theoretical prediction.

approach the theoretical prediction (the dashed lines) as  $K_x$  and  $K_p$  increase. In particular, the upper bound on  $\langle x^2 \rangle_{\rho_{\text{st}}}$  at  $(K_x, K_p) = (7, 7)$  is apparently almost identical to the dashed lines.

However, there are some regions where the numerical bootstrap method does not work well. As energy increases, the upper bound on  $\langle x^2 \rangle_{\rho_{\text{st}}}$  becomes more and more difficult to obtain. Actually, in the original bootstrap method [1], the eigenstates are obtained from lower energy eigenstates [8]. Hence, the bootstrap method may work better in lower energy in general. Besides, the lower bound on  $\langle x^2 \rangle_{\rho_{\text{st}}}$  is also difficult to obtain when the size of the bootstrap matrix size is large. Note that the lower bound in Fig. 4 is the straight line connecting the ground state and the state at  $E = \infty$ . Since handling high energy states may be difficult in the bootstrap method, it might explain why the bootstrap method does not work well for deriving the lower bound.

One interesting feature of this result is that  $\langle x^2 \rangle$  at the energy eigenstates are reproduced as the vertexes of the polygonal region in Fig. 4. Thus, the constraints (2.24) is enough to obtain the energy eigenstates in the bootstrap method. However, this is because  $(E, \langle x^2 \rangle)$  for the eigenstates in the anharmonic oscillator lie on a convex curve, and it does not generally occur. If we change the Hamiltonian and  $(E, \langle x^2 \rangle)$  distribute more complicatedly, some of the eigenstates appear in the inside of the polygon and they cannot be observed. (See, for example,  $(E, \langle x^2 \rangle)$  in the double-well potential shown in Fig. 3.) In order to find the full eigenstates through the bootstrap method, we need to add further constraints to (2.24) as we will see in the next section.

## 2.5 Bootstrapping energy eigenstates

We have investigated the range of the possible values of  $\langle Q \rangle$  in the stationary state, and now we impose further constraints to obtain the energy eigenstates. (This is the original bootstrap method proposed by Han et al [1].) The energy eigenstate  $|E\rangle$  satisfies not only the stationary condition (2.23) but also the following equation

$$\langle E|HO|E\rangle = E\langle E|O|E\rangle \quad (2.25)$$

for any well defined operator  $O$ . Hence, we may obtain the spectrum of the energy eigenstates by evaluating the possible values of  $\langle Q \rangle$  under the constraints,

$$\mathcal{M} \succeq 0, \quad \langle E|HO|E\rangle = E\langle E|O|E\rangle, \quad \langle E|[H, O]|E\rangle = 0, \quad (O \in \{x^m p^n\}). \quad (2.26)$$

Here the constraint  $E = \langle E|H|E\rangle$  in (2.24) is involved in (2.25) with  $O = 1$ . In particular, the constraints (2.23) and (2.25) are quite strong, and they reduce to the following recurrence relation [8, 9, 10, 11],

$$n(n-1)(n-2)\langle x^{n-3} \rangle - 8n\langle x^{n-1}V(x) \rangle + 8nE\langle x^{n-1} \rangle - 4\langle x^nV'(x) \rangle = 0. \quad (2.27)$$

Here we have omitted  $|E\rangle$ . When  $V(x)$  is a polynomial, this recurrence relation can be solved and  $\langle x^n \rangle$  for any integer  $n$  is expressed by a finite number of operators  $\{\langle x^m \rangle\}$  and  $E$ . Similarly,  $\langle x^k p^l \rangle$  for any integers  $k$  and  $l$  is also described by these quantities [8]. Previous studies have shown that these conditions are strong enough to reproduce the observables in the energy eigenstates [1, 6, 8, 9, 10, 12, 13, 14, 15, 16, 17, 18].

### 2.5.1 Example: Anharmonic oscillator

We demonstrate the derivation of the energy eigenstates in the anharmonic oscillator (2.20). In this case, by solving the recurrence relation (2.27), the operator  $\langle x^k p^l \rangle$  is expressed by  $\langle x \rangle$ ,  $\langle x^2 \rangle$  and  $E$ . Then, the bootstrap matrix (2.13) becomes

$$\mathcal{M} = \begin{pmatrix} 1 & \langle x \rangle & 0 & \cdots \\ \langle x \rangle & \langle x^2 \rangle & \frac{i}{2} & \cdots \\ 0 & -\frac{i}{2} & \frac{1}{3}(4E - \langle x^2 \rangle) & \cdots \\ \vdots & \vdots & \vdots & \ddots \end{pmatrix}. \quad (2.28)$$

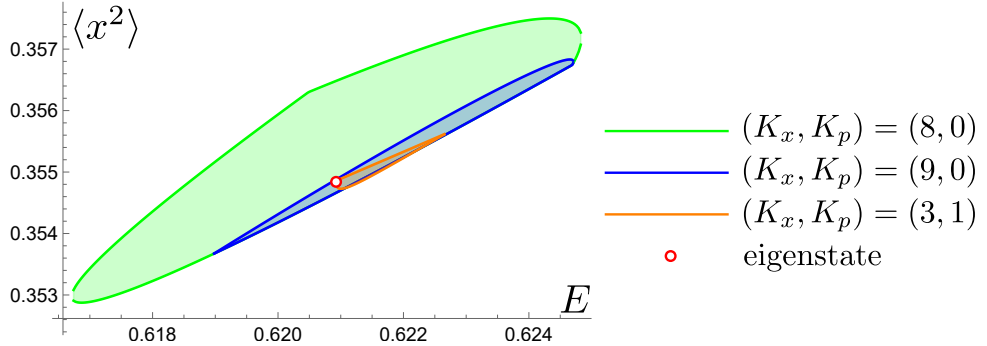


Figure 5: The possible ranges of  $\langle x^2 \rangle$  for the energy eigenstates in the anharmonic oscillator (2.20) near the ground state. The numerical bootstrap method with the constraints (2.26) is solved. The red circle is the result of numerically solving the Schrödinger equation, and the results of the bootstrap method asymptotically approach to it. Similar results can be obtained for other energy eigenstates too, but it works better for lower energies [8].

The constraint  $\mathcal{M} \succeq 0$  for this matrix is quite strong and the allowed regions are point-like. See Fig. 5<sup>9</sup> <sup>10</sup>.

## 2.6 Summary of the one-dimensional problem

Let us summarize the discussions in this section. The bootstrap method allows us to obtain the range of the possible values of observables by applying the various constraints to the expectation values. In particular, the constraints used in this section have the following meanings:

- $\mathcal{M} \succeq 0$ : A generalization of the uncertainty relations.
- $E = \langle H \rangle$ : The state has energy  $E$ .
- $\langle [H, O] \rangle = 0$ : The state is stationary.
- $\langle [H, O] \rangle = 0$  and  $\langle HO \rangle = E \langle O \rangle$ : The state is the energy eigenstate with energy eigenvalue  $E$ .

The first constraint  $\mathcal{M} \succeq 0$  should be satisfied always, and the rest of the constraints specify the states, which we want to investigate.

<sup>9</sup>Our analysis is the same as that of Han et al, with two differences. One is that Han et al took  $K_p = 0$  in (2.12) but we did not. Actually,  $K_p \neq 0$  might improve the numerical analysis [8]. Another difference is that Han et al. imposed  $\langle x \rangle = 0$  by hand, but we did not, although  $\langle x \rangle = 0$  reduces the computational resources. This is because we want to emphasize that the constraint (2.26) is sufficient to obtain the eigenstates. Note that our obtained states satisfy  $\langle x \rangle \simeq 0$ .

<sup>10</sup>The bootstrap matrix linearly depends on  $\langle x \rangle$  and  $\langle x^2 \rangle$  and non-linearly depends on  $E$ . Thus, if we fix  $E$ , the optimization problem (2.26) can be solved by using a linear programming. We solve this problem by using the Mathematica package “SemidefiniteOptimization” and take “DSDP” as the option “Method”.

Note that it was pointed out in [8] that the derivation of the eigenstates in the bootstrap method [1] is related to the Dirac's ladder operator method in harmonic oscillators<sup>11</sup>. Indeed, in the ladder operator problem, the positivity of the expectation value  $\langle E|(a^\dagger)^n(a)^n|E\rangle \geq 0$  and some algebraic relations among the operators are employed, and they may correspond to  $\mathcal{M} \succeq 0$  and other algebraic constraints in the bootstrap method, respectively. Therefore, our results suggest a connection between the Dirac's ladder operator problem and the uncertainty relations.

### 3 Bootstrapping Two-Particle Systems

#### 3.1 Problems in identical particles

Since the bootstrap method efficiently works in the single particle models in one-dimension, it is natural to generalize it to multi-particle systems. However, we will show that some problems arise when the bootstrap method is applied to (indistinguishable) identical particle systems. In order to see it, we consider the following one-dimensional two-particle system,

$$H = \frac{p_1^2}{2} + \frac{p_2^2}{2} + V(x_1, x_2). \quad (3.1)$$

Here  $x_i$  and  $p_i$  are the position and momentum of the  $i$ -th particle ( $i = 1, 2$ ). We impose a condition  $V(x_1, x_2) = V(x_2, x_1)$  on the potential. Then, the energy eigenstate is always symmetric or antisymmetric under the exchange of the two particles  $x_1, p_1 \leftrightarrow x_2, p_2$ . It is also possible that the symmetric and anti-symmetric states degenerate at the same energy level. Related to this property, this model can have three different situations, depending on the statistics of the particles.

- Two identical bose particles  $\Rightarrow$  States are symmetric under the two particle exchange.
- Two identical fermi particles  $\Rightarrow$  States are anti-symmetric under the two particle exchange.
- Two distinct particles  $\Rightarrow$  States are symmetric or anti-symmetric under the two particle exchange.

Note that we do not consider spins. The distinct particle case can be regarded as a system with a flavor symmetry.

Here, we argue whether the bootstrap method correctly derive the physical quantities in each of these three situations. As we have seen in the previous section, in order to specify the desired physical situation in the bootstrap method, we need to impose appropriate constraints on expectation

---

<sup>11</sup>We can easily show that, when we take  $\tilde{O} = \sum_n b_n(a^\dagger)^n$  in (2.9) in the harmonic oscillator (2.2), the bootstrap problem (2.26) reduces to the Dirac's ladder operator problem [8].

values. In the case of the identical particles, physical quantities are invariant under the exchange of the two particles  $x_1, p_1 \leftrightarrow x_2, p_2$ , while they need not be invariant in the case of the distinct particles. Hence, we impose the constraint

$$\langle O(x_1, x_2, p_1, p_2) \rangle = \langle O(x_2, x_1, p_2, p_1) \rangle \quad (3.2)$$

in the identical particle case, and we do not impose it in the distinct particle case.

In the case of the identical particles, we need to further distinguish the bosons and fermions. However, the bootstrap method cannot do it. This is because the quantities considered in the bootstrap method are only expectation values, which are always invariant under the exchange of the particles as in (3.2). If the bootstrap method could handle amplitudes or wave functions, it would be possible to distinguish the bosons and fermions, since their sign are flipped under the particle exchange in the case of the fermions. However, there is currently no known way to treat these quantities in the bootstrap method. Therefore, the bootstrap method cannot distinguish the bosons and fermions. Hence, the bootstrap method may be applicable to the identical particles but the predictions would be limited.

On the other hand, the bootstrap method may work properly in the distinct particle case.

### 3.1.1 Example 1: Non-interacting harmonic oscillators

To see the problem of two-particle systems in the bootstrap method concretely, we investigate two non-interacting harmonic oscillators,

$$H = \sum_{i=1}^2 \frac{1}{2} p_i^2 + \frac{1}{2} x_i^2. \quad (3.3)$$

We discuss the derivation of the bounds on  $\langle x_1 \rangle$  under the constraint  $E = \langle H \rangle$ . As we show in Appendix A.4, by using the property that the harmonic oscillators are quadratic, the bounds are given as

$$\text{Two distinct particles: } \langle x_1 \rangle^2 \leq 2(E - \hbar), \quad (3.4)$$

$$\text{Two identical bose particles: } \langle x_1 \rangle^2 \leq E - \hbar, \quad (3.5)$$

$$\text{Two identical fermi particles: } \langle x_1 \rangle^2 \leq E - 2\hbar. \quad (3.6)$$

However, since this derivation is limited to quadratic systems, it is desirable to reproduce these results employing the uncertainty relation. (If the uncertainty relation works, we can expect that the bootstrap method, which generalizes the uncertainty relation, may be used for more general systems.)

Similar to the derivation (2.3) in the single particle problem, the condition  $E = \langle H \rangle$  and the uncertainty relation lead to the inequality,

$$\langle x_1 \rangle^2 + \langle x_2 \rangle^2 \leq 2(E - \hbar). \quad (3.7)$$

If the two particles are distinguishable,  $\langle x_1 \rangle$  and  $\langle x_2 \rangle$  are independent, and we obtain the bound

$$\langle x_1 \rangle^2 \leq 2(E - \hbar). \quad (3.8)$$

This reproduces (3.4), and thus the uncertainty relation (and the bootstrap method) may work for the distinct particles. On the other hand, if the two particles are identical and not distinguishable, the relation  $\langle x_1 \rangle = \langle x_2 \rangle$  is held through (3.2), and (3.7) becomes

$$\langle x_1 \rangle^2 \leq E - \hbar. \quad (3.9)$$

No further restrictions can be imposed from the uncertainty relation. This result is consistent with the boson (3.5), but not with the fermion (3.6). Clearly, the bound (3.9) is weaker than the desired bound (3.6) for the fermions. This means that the condition obtained from the uncertainty relation is not strong enough. This is due to the fact that, as mentioned earlier, the uncertainty relation handles only expectation values, which do not distinguish bosons and fermions.

Similar problems must appear in more general models in the bootstrap methods too. The related issues would also arise in the derivation of the energy eigenstates. We will consider this problem in the next subsection.

### 3.1.2 Example 2: Yang-Mills quantum mechanics

As the second example, we study so called “Yang-Mills quantum mechanics” (YMQM), which is not free and known to show chaos [19, 20, 21],

$$H = \frac{p_1^2}{2} + \frac{p_2^2}{2} + x_1^2 x_2^2. \quad (3.10)$$

Numerical computation of the Schrödinger equation yields symmetric and antisymmetric eigenfunctions. There are also cases where both degenerate. In order to compute the observables such as  $\langle x_1^2 \rangle$ , we need to select the eigenfunctions depending on the three situations: the distinct particles, the bosonic identical particles and the fermionic identical particles. The plots of  $(E, \langle x_1^2 \rangle)$  in these cases are shown in Fig. 6 for the distinct particles and Fig. 7 for the identical particles. Note that, in the case of the distinct particles, when two eigenstates degenerate, superpositions of these two are allowed, and the expectation values of  $\langle x_1^2 \rangle$  at this energy level take various values

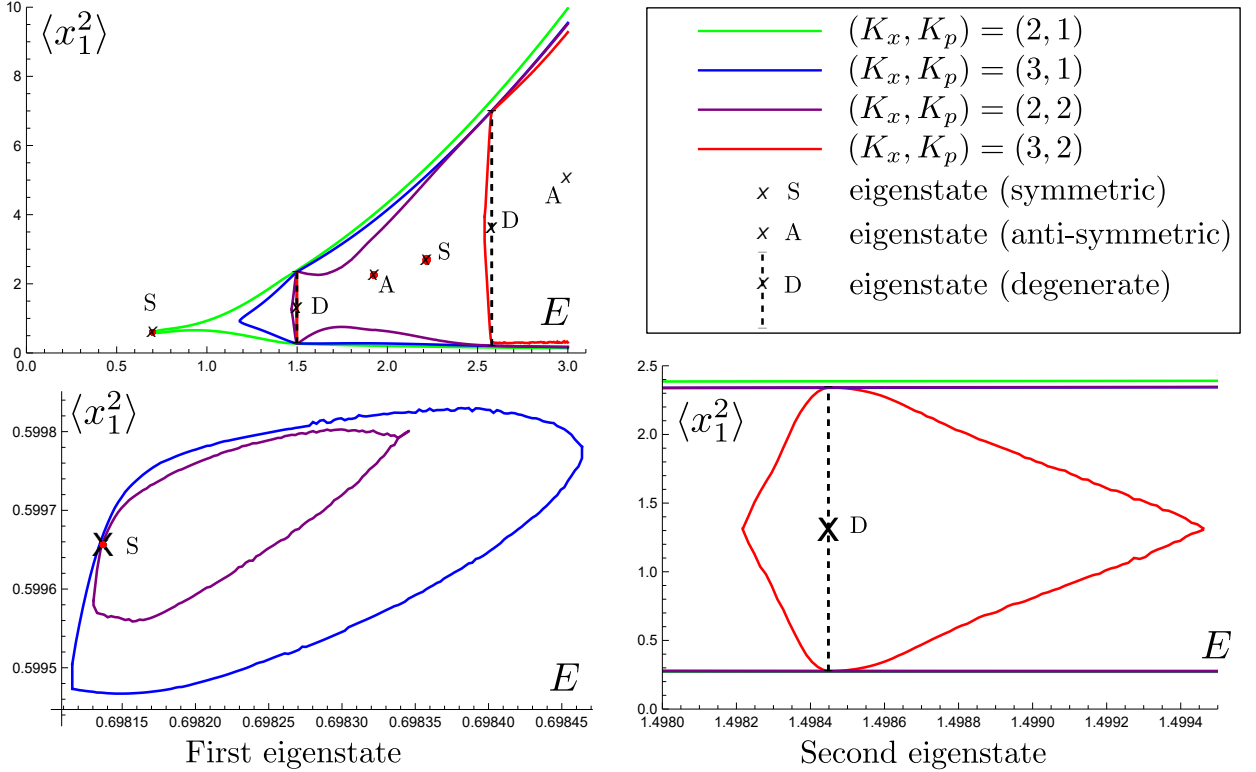


Figure 6: Energy eigenstates for the distinct two-particles in the YMQM (3.10). “ $\times$ ” denotes the eigenstates obtained by solving the Schrödinger equation numerically. The lower left and the lower right figures are the neighborhood of the first and second eigenstates in the upper left panel, respectively. The eigenstates are symmetric or antisymmetric with respect to the exchanges of the particles. In particular, when these two states degenerate,  $\langle x_1^2 \rangle$  can take various values due to their superpositions. This range is indicated by the vertical dashed lines in the figures. It can be seen that the bootstrap method reproduces these eigenstates including the superpositions as  $K_x$  and  $K_p$  increase. Particularly, the first eigenstate at  $(K_x, K_p) = (3, 2)$  (the red “dot”) is almost point-like. However, the bootstrap method cannot indicate whether these eigenstates are symmetric or antisymmetric.

within a certain range. The black vertical dashed lines in Fig. 6 indicate this range. On the other hand, in the case of the identical particles, we need to exclude the anti-symmetric states or the symmetric states according to whether the particles are bosons or fermions, and the degeneracy does not occur.

Now, let us see if the bootstrap method can reproduce these eigenstates. We take the seed operator

$$\tilde{O} = \sum_{k,l=0}^{K_x} \sum_{m,n=0}^{K_p} b_{klmn} x_1^k x_2^l p_1^m p_2^n, \quad (3.11)$$

and construct the bootstrap matrix from it. Then, we solve the optimization problem (2.26), which

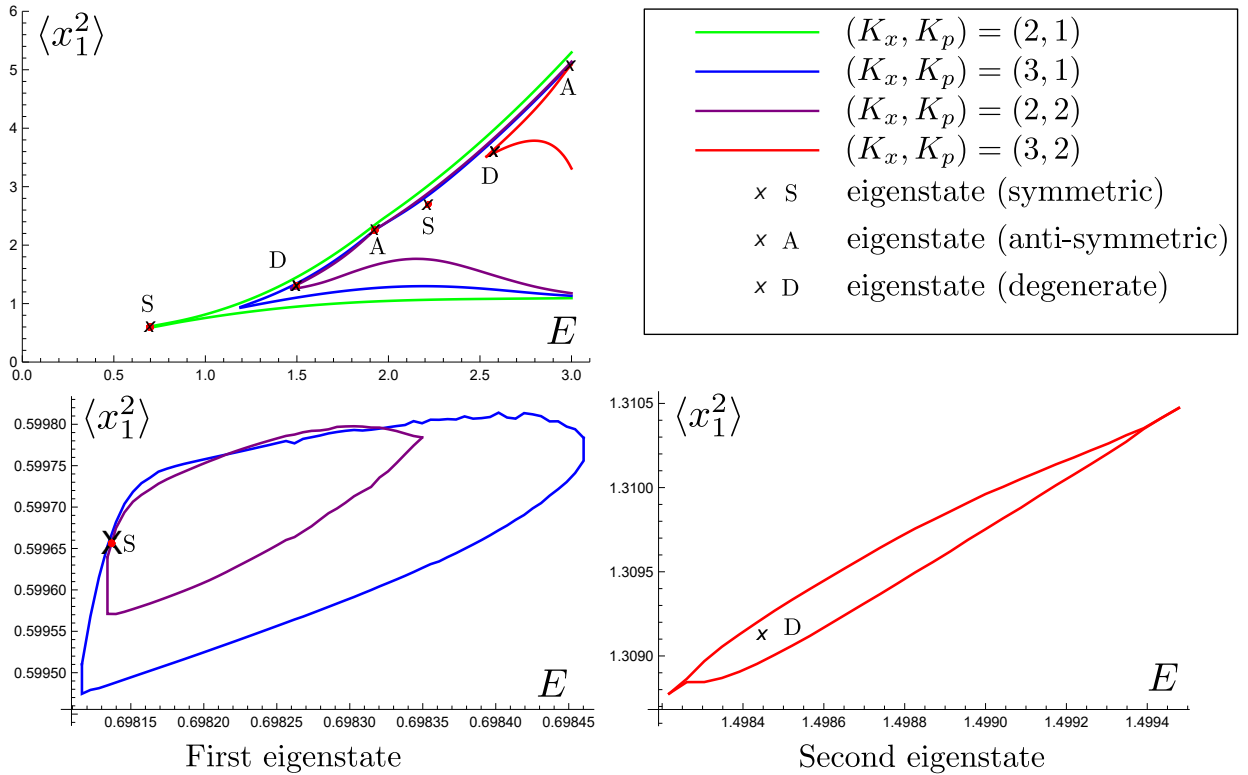


Figure 7: Energy eigenstates for the identical two-particles in the YMQM (3.10) through the numerical bootstrap method. “ $\times$ ” denotes the eigenstates obtained by solving the Schrödinger equation numerically. The lower left and the lower right figures are the neighborhood of the first and second eigenstates in the upper left panel, respectively. The eigenstates are symmetric or antisymmetric with respect to the particle exchanges, and we take either of them depending on whether the particles are the bosons or the fermions. At the degenerate states, the bosons and fermions have the same values  $\langle x_1^2 \rangle$ . Different from the distinct particle case, their superposition is not allowed, since we take only one state. It can be seen that the bootstrap method reproduces these states as  $K_x$  and  $K_p$  increase. The first eigenstate at  $(K_x, K_p) = (3, 2)$  is again almost point-like. However, the bootstrap method cannot indicate whether the states are symmetric or antisymmetric.

is linear if we fix  $E$ . We also impose the constraints (3.2) of the particle exchanges in the identical particle case. The numerical results are illustrated in Fig. 6 (the distinct particles) and Fig. 7 (the identical particles)<sup>12</sup>. They show that, for both identical and distinct particles, the range of the possible values of  $\langle x_1^2 \rangle$  tends to approach to the eigenstates as  $K_x$  and  $K_p$  increase. The numerical bootstrap method also reproduces the range of  $\langle x_1^2 \rangle$  due to the degeneracy in the distinct particle case.

However, as we have discussed, it is not possible to determine whether the obtained eigenstates are for the bosons or for the fermions through the bootstrap method. (We can only say that there are states corresponding to the bosons and the fermions at the degenerate states from the results for the distinct particles.) Therefore, the bootstrap method has only limited predictive power for the identical particle case.

Note that the number of the independent variables in the bootstrap matrix  $\mathcal{M}$  in the YMQM increases as  $K_x$  and  $K_p$  increases, and it is more than 400 at  $(K_x, K_p) = (3, 2)$  even after we impose the constraints in (2.26). In contrast, in the case of the one-dimensional anharmonic oscillator argued in Sec. 2.5.1, the independent variables are only two:  $\langle x \rangle$  and  $\langle x^2 \rangle$ , and it does not change by  $(K_x, K_p)$  because of the strong constraint (2.27). Thus, the numerical bootstrap analysis in the YMQM case is qualitatively different from the anharmonic oscillator case, and our results show that the method works even in such a case.

### 3.1.3 Bootstrapping other states with $E = \langle H \rangle$ in YMQM

As we have studied in the one-dimensional quantum mechanics, the bounds on the possible values of observables for general mixed states with energy  $E = \langle H \rangle_\rho$  in the YMQM will be derived through the bootstrap method. We solve the optimization problem (2.19) with the Hamiltonian (3.10) by using the bootstrap matrix constructed from the operator (3.11). The results for  $\langle x_1 \rangle$  and  $\langle x_1^2 \rangle$  are illustrated in Fig. 8 and Fig. 9, respectively<sup>13</sup>. It seems that  $\langle x_1^2 \rangle$  have not converged yet.  $\langle x_1 \rangle$  in the distinct particle case also have not converged yet, since they do not satisfy  $\langle x_1 \rangle^2 < \langle x_1^2 \rangle$  for larger  $E$  as shown in Fig. 9. (Another possibility is that the obtained  $\langle x_1^2 \rangle$  in this region is numerically wrong.) They might have converged for smaller  $E$ .  $\langle x_1 \rangle$  in the identical particle case might have converged too. In order to obtain the convergent results, we need to perform numerical

---

<sup>12</sup>We solve this problem by using the Mathematica package “SemidefiniteOptimization” with the option “Mosek” and “CSDP”. In our numerical analysis, sometimes unnatural line-like regions were observed. In these regions, the bootstrap matrices have much larger negative eigenvalues, which mean the condition  $\mathcal{M} \succeq 0$  is not satisfied and the data would be not reliable. In our figures, we have removed these regions.

<sup>13</sup>In our analysis in this subsection, we use the Mathematica package “SemidefiniteOptimization” with the option “DSDP”.

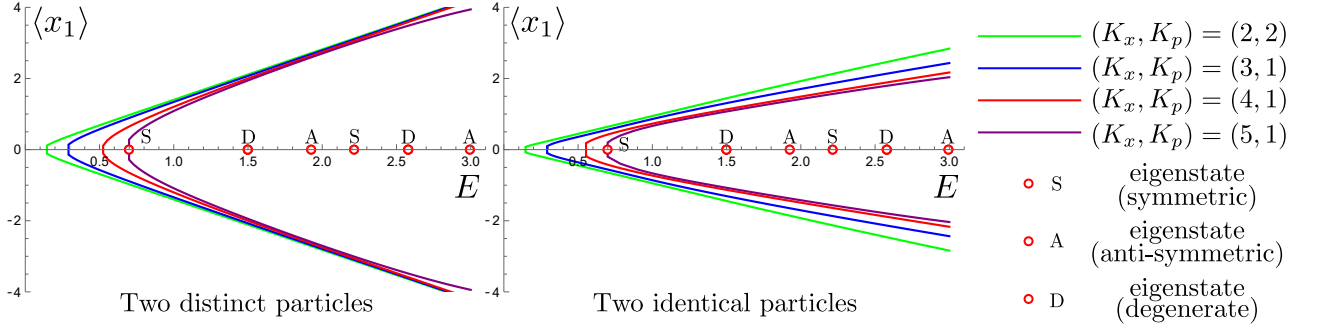


Figure 8: The possible ranges of  $\langle x_1 \rangle$  in the YMQM for general mixed states with  $E = \langle H \rangle$ . The left panel is for the distinct particles and the right panel is for the identical particles in which the constraint (3.2) is imposed. Thus, the region in the right panel is smaller.

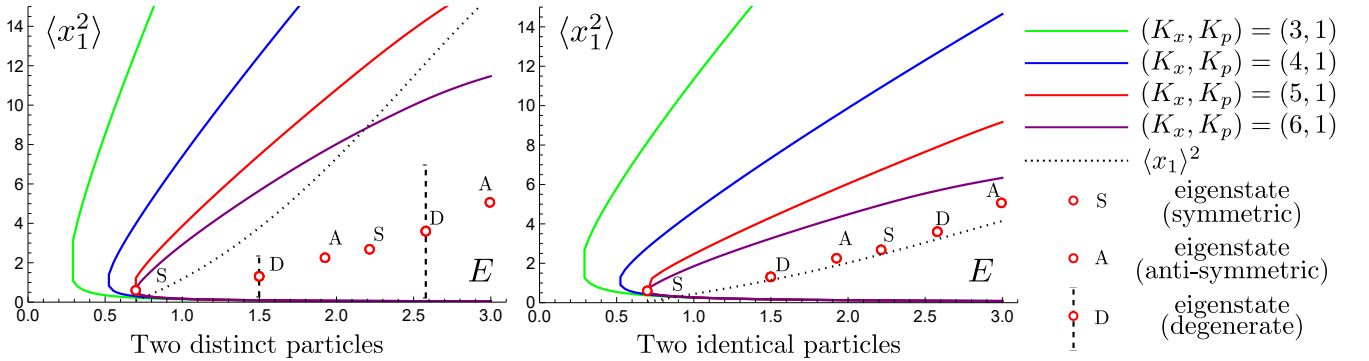


Figure 9: The possible ranges of  $\langle x_1^2 \rangle$  in the YMQM for general mixed states with  $E = \langle H \rangle$ . The left panel is for the distinct particles and the right panel is for the identical particles. It seems that the bootstrap results have not converged yet at  $(K_x, K_p) = (6, 1)$ . We also plot  $\langle x_1 \rangle^2$  at  $(K_x, K_p) = (5, 1)$ , which is obtained from the data in Fig. 8. We see that  $\langle x_1^2 \rangle > \langle x_1 \rangle^2$  is not satisfied for larger  $E$  in the distinct particle case. It is an evidence that the analysis for  $\langle x_1 \rangle$  have not been converged yet. Taking larger  $K_x$  and  $K_p$  might improve it.

analysis for larger  $K_x$  and  $K_p$ , but, due to our limited computational resources, we leave it as a future works.

We also investigate stationary states with energy  $E = \langle H \rangle_{\rho_{\text{st}}}$  by solving the constraint (2.24). The results for  $\langle x_1^2 \rangle_{\rho_{\text{st}}}$  are shown in Fig. 10<sup>14</sup>.

In all of the bootstrap results in this subsection, the regions in the identical particle case are always smaller than those in the distinct particle case because of the additional constraint (3.2). In the identical particle case, the actual allowed regions must be smaller than the obtained regions in our analysis, similar to the harmonic oscillator case discussed in 3.1.1. Particularly, the region for

<sup>14</sup>To improve the numerical analysis for stationary states, we impose the parity condition  $\langle x_1^k x_2^l p_1^m p_2^n \rangle = 0$  if either  $k+m$  or odd  $l+n$  is odd.

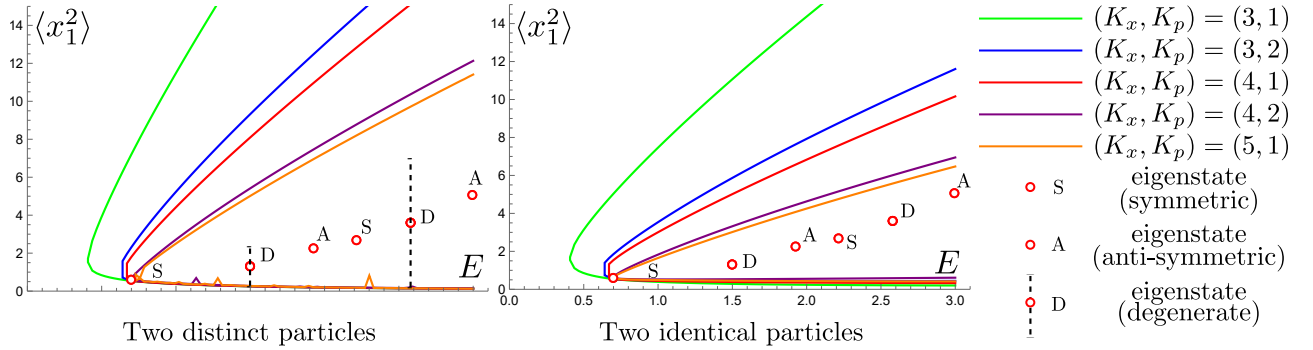


Figure 10: The possible ranges of  $\langle x_1^2 \rangle$  in the YMQM for stationary states with  $E = \langle H \rangle$ .

the fermions should start from the ground state, but the bootstrap method cannot show it at all.

Note that the YMQM (3.10) has flat directions along the line  $x_1 = 0$  and  $x_2 = 0$ . Thus,  $x_1$  or  $x_2$  can take arbitrary large values even at zero energy in classical mechanics. On the other hand, in quantum mechanics, the probability of taking such a large value  $x_i$  is expected to be small due to the uncertainty relation [22]. Our results for  $\langle x_1 \rangle$  and  $\langle x_1^2 \rangle$  explicitly support this prediction.

In this section, we have discussed the application of the bootstrap method to two-particle systems in one-dimension. In the case of the identical particles, the bootstrap method has only limited predictive power. On the other hand, it properly works when the two particles are distinct. In this case,  $x_1$  and  $x_2$  can be interpreted as “the coordinates of one particle in two dimensions” instead of “the coordinates of two particles in one dimension.” Therefore, the bootstrap method works even in two dimension system. By increasing the number of degrees of freedom in this way, we expect that it will also work for multi-particles in one or higher dimensions.

## 4 Bootstrapping Thermal Equilibrium States

In the previous section, we have presented that the bootstrap method also works for multi-particle systems, although it is limited for identical particles. An interesting question in multi-particle systems is whether the bootstrap method can predict physical quantities in thermal equilibrium. In this section, we discuss this problem. To make the problem concrete, we consider an  $N$ -particle system ( $N \gg 1$ ) with Hamiltonian

$$H = \frac{1}{2} \sum_{i=1}^N p_i^2 + U(x_1, x_2, \dots, x_N), \quad (4.1)$$

where  $x_i$  is the position of the  $i$ -th particle and  $p_i$  is its conjugate momentum.  $U(x_1, x_2, \dots, x_N)$  is a potential and we assume that it is symmetric with respect to the particle exchanges. (The large- $N$  matrix models studied in [1] are examples of this model.) In this model, issues of identical particles would exit. In addition, there is another problem that, in principle, it is difficult to handle temperature and entropy in the bootstrap method. In this section, we first introduce this problem in Sec. 4.1, and after that we will discuss issues on the identical particles in Sec. 4.2. However, if the system is integrable, the bootstrap method may exceptionally work. We will argue it in Sec. 4.3.

#### 4.1 Difficulties in bootstrapping canonical ensemble

In this section, we try to apply the bootstrap method to the model (4.1) in thermal equilibrium with temperature  $T$ . Such a state is described by the stationary mixed state (2.22) with the Boltzmann factor  $c_n = \exp(-\beta E_n)/Z$ , and the expectation value of an observable  $O$  is given by

$$\langle O \rangle_\beta := \frac{1}{Z} \sum_n e^{-\beta E_n} \langle n | O | n \rangle, \quad Z := \sum_n \langle n | e^{-\beta H} | n \rangle. \quad (4.2)$$

Here  $\beta := 1/T$  and we have taken the Boltzmann constant 1. Typically, we will take  $O$  as an averaged macroscopic quantity, for example,

$$\overline{x^m p^n} := \frac{1}{N} \sum_{i=1}^N x_i^m p_i^n. \quad (4.3)$$

In order to evaluate physical quantities in this thermal equilibrium state using the bootstrap method, constraints that specify this state should be imposed on quantities  $\langle O \rangle_\beta$ . Since thermal equilibrium state is a kind of stationary mixed states, the constraint (2.23) should be imposed. Then, we need to find additional constraints such that we distinguish the thermal equilibrium state from general stationary mixed states.

We notice that the thermal equilibrium state (4.2) satisfies the condition,

$$\frac{\partial}{\partial \beta} \langle O \rangle_\beta = \langle H \rangle_\beta \langle O \rangle_\beta - \langle HO \rangle_\beta. \quad (4.4)$$

(We can also find similar equations for the higher-order derivative of  $\beta$ .) However, this condition is a differential equation with respect to  $\beta$ , which is not useful at all in the bootstrap method<sup>15</sup>. On the other hand, this relation gives us indirectly useful information. That is, when the system size is large, the expectation values of averaged observables such as (4.3) should be factorized,

$$\langle O_1 O_2 \rangle_\beta = \langle O_1 \rangle_\beta \langle O_2 \rangle_\beta + O(1/N). \quad (4.5)$$

---

<sup>15</sup>Since the relation (4.4) is a differential equation, if we know the expectation value  $\langle O \rangle_\beta$  at a certain temperature, we may use it to evaluate the physical quantity at a slightly different temperature  $\beta + \Delta\beta$ . On the other hand, the bootstrap method is not so useful in combination with differential equations, because it is a method to test whether the expectation values  $\langle O \rangle_\beta$  is consistent with the various constraints.

Since  $\langle O_1 \rangle$  and  $\langle O_2 \rangle$  would be  $O(1)$  quantities, we may ignore the second term on the right-hand side. If this relation does not hold, the order of  $N$  does not match on the right and left-hand sides of the equation (4.4). Therefore, such factorization must occur in the thermal equilibrium state (4.2). (Conversely, factorization does not need to occur in general stationary mixed states.) In fact, in statistical mechanics, such a relation is naturally expected from the central limit theorem. In addition, in large- $N$  gauge theories, such a relation is also expected as large- $N$  factorizations<sup>16</sup>. So, the factorization (4.5) is one of the conditions that distinguish the thermal equilibrium state from general stationary mixed states.

Note that, once we impose the factorization condition (4.5), the commutator relation (2.23) seems trivial. However, it provides important relations at  $O(1/N)$ , and we pick them up when we use the bootstrap method. Similar things happen in the relation (4.4) too, although we will not use (4.4) in our bootstrap analysis.

We could not find any other useful conditions, which characterize the thermal equilibrium state. In particular, the factorization condition (4.5) has no information on temperature. This implies that temperature cannot be handled in the bootstrap method. In other words, it is difficult for the bootstrap method to predict the expectation values of observables at a given temperature. (The only exception is the ground state corresponding to zero-temperature.)

Related to the difficulty of handling temperature in the bootstrap method, chemical potentials cannot be handled either. These results suggest that the bootstrap method has difficulty in dealing with (grand) canonical ensembles specified by temperature and chemical potentials.

## 4.2 Bootstrapping micro-canonical ensemble

We have seen that it is difficult to investigate the temperature dependence in thermal equilibrium using the bootstrap method. However, the bootstrap method allows us to specify energy as  $E = \langle H \rangle$ . Therefore, there is a possibility to evaluate physical quantities in thermal equilibrium as a microcanonical ensemble. Specifically, we impose the following constraints,

$$\mathcal{M} \succeq 0, \quad E = \langle H \rangle, \quad \langle [H, O] \rangle = 0, \quad \langle O_1 O_2 \rangle = \langle O_1 \rangle \langle O_2 \rangle, \quad (4.6)$$

and investigate the range of possible values of  $\langle Q \rangle$ . If the obtained range is sufficiently narrow, the value  $\langle Q \rangle$  may correspond to that of the micro-canonical ensemble at the given energy  $E$ .

However, recall that the bootstrap method cannot distinguish the two bosons and two fermions in the two particle systems. For the  $N$ -particle system, there are much more possibilities on the

---

<sup>16</sup>Large- $N$  factorizations do not need to occur in arbitrary states in large- $N$  gauge theories.

particle species such as multiple species of bosons and fermions. Then, it may be difficult to obtain convergent results through the bootstrap method which cannot distinguish them.

In addition, even if we obtain some reliable and convergent results, the bootstrap method cannot give us the entropy. This is because the bootstrap method only tells us whether the value of a physical quantity is consistent with quantum mechanics or not, and it does not tell us the degeneracy.

### 4.3 Bootstrapping free particles in micro-canonical ensembles

So far, we have discussed the difficulties on the bootstrap method for thermal equilibrium states. It can be applied to micro-canonical ensembles only, and, even in this case, the results may not converge. However, we show a possibility that the bootstrap method can derive convergent results for micro-canonical ensembles in integrable systems.

In integrable systems, there are numerous conserved charges, and thermal equilibrium states are specified by these charges or their chemical potentials. (The ground canonical ensemble characterized by these numerous chemical potentials is called “generalized Gibbs ensemble” (GGE) [2], and are actively studied recently. See review articles [23, 24].) We show that, in the micro-canonical ensemble, the numerous conserved charges may fix the physical quantities in the bootstrap method.

In order to see it, we consider two examples: non-interacting  $N$  harmonic oscillators and non-interacting  $N$  anharmonic oscillators.

#### 4.3.1 Example 1: Non-interacting $N$ harmonic oscillators

We investigate the non-interacting  $N$  harmonic oscillators in one-dimension,

$$H = \hbar \sum_{i=1}^N a_i^\dagger a_i, \quad a_i = \frac{1}{\sqrt{2\hbar}} (x_i + ip_i). \quad (4.7)$$

This system has the infinite number of the conserved charges,

$$R_m := \frac{1}{N} \sum_{i=1}^N (a_i^\dagger)^m a_i^m, \quad m = 2, 3, \dots. \quad (4.8)$$

Hence, thermal equilibrium states of this model in the micro-canonical ensemble are specified by  $E = \langle H \rangle$  and  $r_m := \langle R_m \rangle$ .

We will show that observables such as  $\langle \overline{x^m p^n} \rangle$  in the thermal equilibrium states can be determined by the bootstrap method. By regarding the conserved charges (4.8), we modify the constraints (4.6) for the micro-canonical ensemble as,

$$\mathcal{M} \succeq 0, \quad E = \langle H \rangle, \quad \langle [H, O] \rangle = 0, \quad r_m = \langle R_m \rangle, \quad \langle O_1 O_2 \rangle = \langle O_1 \rangle \langle O_2 \rangle. \quad (4.9)$$

What we should do is finding the possible values of  $\langle \overline{x^m p^n} \rangle$  which are consistent with these constraints. Actually, we can solve this problem analytically. We define the operators  $R_{mn} := \frac{1}{N} \sum_{i=1}^N (a_i^\dagger)^m (a_i)^n$  and substitute it to the constraint  $\langle [H, O] \rangle = 0$  in (4.9), and obtain

$$0 = \langle [H, R_{mn}] \rangle = (m - n) \langle R_{mn} \rangle. \quad (4.10)$$

Hence,  $\langle R_{mn} \rangle = 0$  if  $m \neq n$ . Since the observable  $\langle \overline{x^m p^n} \rangle$  can be expressed by a sum of  $\langle R_{kl} \rangle$ , the value of  $\langle \overline{x^m p^n} \rangle$  is determined by  $\langle R_{11} \rangle = E$  and  $\langle R_{kk} \rangle = r_k$ . Therefore, the observables in this system in thermal equilibrium are completely fixed by the conserved charges  $E$  and  $\{r_m\}$ .

Note that we have used the constraint  $\langle [H, O] \rangle = 0$  and  $r_m = \langle R_m \rangle$  only. Here we comment on the remaining constraints in (4.9). It is easy to show that the constraint  $\langle O_1 O_2 \rangle = \langle O_1 \rangle \langle O_2 \rangle$  is automatically satisfied in free particle systems, if we consider the averaged operators such as (4.3) and take  $N$  large. (It implies that any stationary states of one-dimensional free particles are always thermal equilibrium states.) Besides, the constraint  $\mathcal{M} \succeq 0$  is satisfied, if we take appropriate conserved charge  $E$  and  $\{r_m\}$ . Thus, this can be regarded as an “initial value problem”<sup>17</sup>. One way to generate suitable conserved charges is using a bose or fermi distribution function, which we will demonstrate in the next example.

#### 4.3.2 Example 2: Non-interacting $N$ anharmonic oscillator

Since the harmonic oscillator (4.7) is so simple that we can solve it analytically, as a more nontrivial example, we consider non-interacting  $N$  anharmonic oscillators,

$$H = \sum_{i=1}^N h_i, \quad h_i := \frac{1}{2} p_i^2 + \frac{1}{2} x_i^2 + \frac{1}{4} x_i^4. \quad (4.11)$$

Then, the system has the conserved charges,

$$H^{(m)} := \frac{1}{N} \sum_{i=1}^N h_i^m, \quad m = 1, 2, 3, \dots. \quad (4.12)$$

Here  $H^{(1)}$  is the Hamiltonian (4.11).

By using the numerical bootstrap method, we seek the possible range of the expectation value of the observable

$$\overline{x^2} := \frac{1}{N} \sum_{i=1}^N x_i^2 \quad (4.13)$$

---

<sup>17</sup>The issue of the particle species also reduces to the initial value problem. Namely, we need to prepare suitable charges, which are consistent with the given particle species.

in this system at thermal equilibrium. Hence, we derive the upper and lower bounds on  $\langle \bar{x}^2 \rangle$  under the constraints,

$$\mathcal{M} \succeq 0, \quad \langle [H, O] \rangle = 0, \quad E^{(m)} := \langle H^{(m)} \rangle, \quad \langle O_1 O_2 \rangle = \langle O_1 \rangle \langle O_2 \rangle. \quad (4.14)$$

Here  $\langle O_1 O_2 \rangle = \langle O_1 \rangle \langle O_2 \rangle$  is automatically satisfied at large- $N$  as we mentioned in the previous section.

We construct the bootstrap matrix  $\mathcal{M}$  as follows. Since we are interested in the averaged operator  $\bar{x}^2$  (4.13), it is useful to take the seed operator

$$\tilde{O}_i := \sum_{m=0}^{K_x} \sum_{n=0}^{K_p} b_{mn} x_i^m p_i^n. \quad (4.15)$$

Then  $\sum_{i=1}^N \langle \tilde{O}_i^\dagger \tilde{O}_i \rangle \geq 0$  is satisfied for any  $\{b_{mn}\}$ , and we obtain the bootstrap matrix  $\mathcal{M}$  (2.13) where  $\langle x^m p^n \rangle$  are replaced by  $\langle \bar{x}^m \bar{p}^n \rangle$ . In addition,  $H^{(m)}$  can be expressed by  $\bar{x}^k \bar{p}^l$  too. Then, all the variables in the constraints (4.14) are expressed by the averaged operators  $\bar{x}^k \bar{p}^l$ , and we do not need to handle the operators for the individual particle such as  $x_i$  and  $p_j$  anymore. In this way, the constraints (4.14) become formally equivalent to the constraints (2.24) for the single anharmonic oscillator with the additional constraints  $E^{(m)} = \langle H^{(m)} \rangle$  ( $m = 2, 3, 4, \dots$ ) by identifying  $\bar{x}^m \bar{p}^n$  and  $x^m p^n$ . This is a strong simplification, and is one advantage of the bootstrap analysis. (Related simplifications in the bootstrap method in multi-particle systems are expected, and several works on large- $N$  gauge theories have been done [1, 25, 26, 27, 28].)

Before solving the bootstrap problem (4.14), we need to prepare suitable conserved charges  $E$  and  $\{E^{(m)}\}$ . For this purpose, we assume that the  $N$  particles are all the same boson and they obey the standard bose distribution function with temperature  $T = 1/\beta$  and chemical potential  $\mu$ .<sup>18</sup> Then the expectation value of the operator  $\bar{x}^m \bar{p}^n$  in the thermal equilibrium state is given by

$$\langle \bar{x}^m \bar{p}^n \rangle_{\beta, \mu} := \frac{1}{N(\beta, \mu)} \sum_{n=0}^{\infty} \frac{1}{e^{\beta(e_n - \mu)} - 1} \langle n | x^m p^n | n \rangle, \quad (4.16)$$

$$N(\beta, \mu) := \sum_{n=0}^{\infty} \frac{1}{e^{\beta(e_n - \mu)} - 1}. \quad (4.17)$$

Here  $|n\rangle$  is the energy eigenstate for the single particle and  $e_n$  is its energy eigenvalue.  $N(\beta, \mu)$  is the number of the bose particles. Then, through (4.12), we obtain  $E^{(m)}$ ,

$$E^{(m)}(\beta, \mu) = \frac{1}{N(\beta, \mu)} \sum_{n=0}^{\infty} \frac{(e_n)^m}{e^{\beta(e_n - \mu)} - 1}, \quad (m = 1, 2, \dots). \quad (4.18)$$

---

<sup>18</sup>This system has infinite number of chemical potentials corresponding to the conserved charges (4.12). If we take these chemical potentials zero except those corresponding to  $E$  and  $N$ , we obtain the standard bose distribution function in (4.17).

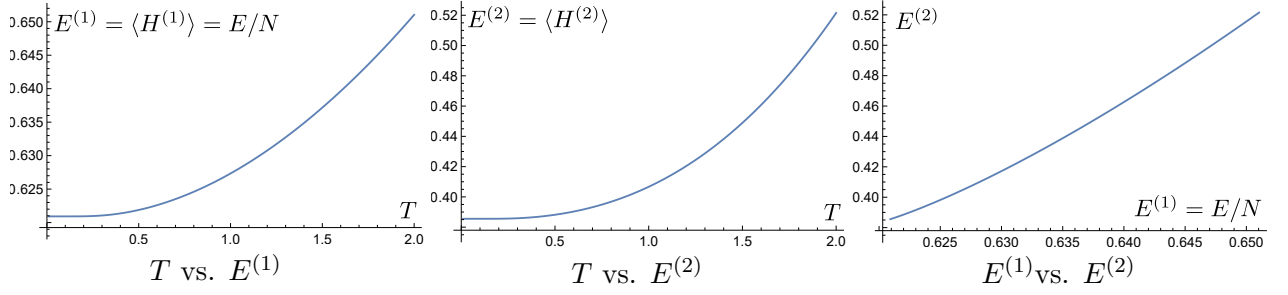


Figure 11: Temperature dependence of  $E^{(1)} = E/N$  and  $E^{(2)}$  for the  $N$  bosе particles in the anharmonic oscillator (4.11). We take  $N = 100$ . Through the plots of  $T$  vs.  $E^{(1)}$  and  $T$  vs.  $E^{(2)}$ , by eliminating  $T$ , we obtain the plot of  $E^{(1)}$  vs.  $E^{(2)}$ .

In order to obtain the observables in the micro-canonical ensemble at given  $E$  and  $N$ , we tune  $T$  and  $\mu$  such that  $E = E(\beta, \mu)$  and  $N = N(\beta, \mu)$  in the ground canonical ensemble. Then, by using these tuned  $T$  and  $\mu$ , we obtain  $E^{(m)}(E, N)$  and  $\langle \bar{x^m p^n} \rangle(E, N)$ . Particularly, we will use  $E^{(m)}(E, N)$  as the input of the bootstrap analysis in (4.14), and test whether  $\langle \bar{x^m p^n} \rangle(E, N)$  is reproduced.

In our numerical analysis, we take  $N = 100$  and first fix  $\mu(\beta, N)$  through (4.17) for each  $\beta$ . Then, we compute the temperature dependence of  $E$  and  $E^{(2)}$  at  $N = 100$  as shown in Fig. 11. From these results, by eliminating temperature, we obtain  $E^{(2)}(E, N)$  as shown in Fig. 11 (right panel). Similarly, we plot  $\langle \bar{x^2} \rangle(E, N)$  in Fig. 12.

We perform the numerical bootstrap analysis by using this  $E^{(m)}(E, N)$  in the constraint (4.14). Actually, we find that just  $E^{(2)}$  is sufficient to reproduce  $\langle \bar{x^2} \rangle(E, N)$ . The results are shown in Fig. 12<sup>19</sup>. We find that they are consistent with the thermal equilibrium state (4.16).

However, the bootstrap method does not work properly in higher energy region  $E/N > 0.65$ . Since the ground energy is  $E/N = 0.6209$ , the region, in which the bootstrap method works, is very low energy. We guess that it may be a technical issue. Note that we can do in principle similar analysis for  $N$  fermions by using the fermi distribution function in (4.17). However, the fermi energy is high at large  $N$ , and we need to handle higher energy, which would be difficult in the bootstrap method. Indeed, as far as we tried, we could not obtain reliable results through the bootstrap analysis. Improvement of numerical method might resolve these issues.

#### 4.3.3 Thermometer?

We have seen that the bootstrap method can reproduce physical quantities at thermal equilibrium in the integrable systems. However, as discussed in the previous section, temperature and entropy

<sup>19</sup>We solve this problem by using the Mathematica package “SemidefiniteOptimization” with the option “Mosek”. There, we imposed the parity condition  $\langle \bar{x^m p^n} \rangle = 0$ , ( $n + m$  : odd) in order to perform the numerical analysis efficiently.

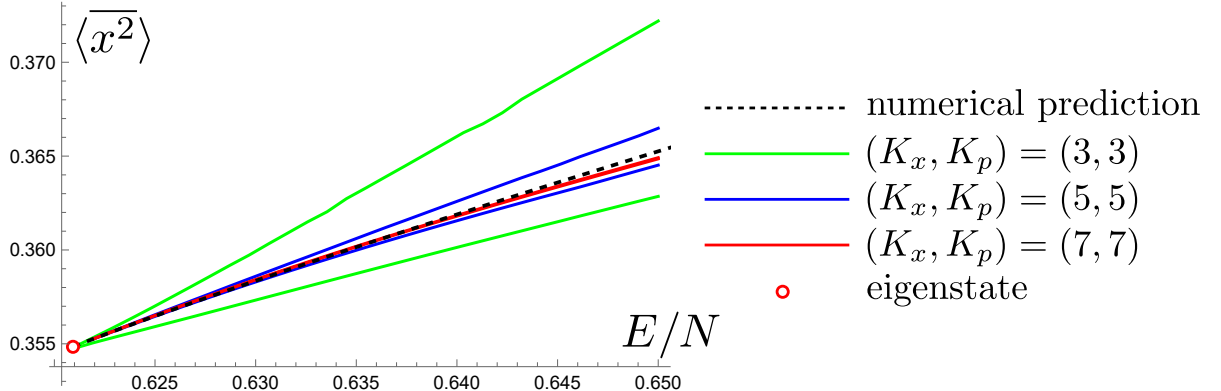


Figure 12:  $E$  vs.  $\langle \overline{x^2} \rangle$  for the  $N$  boson particles in the anharmonic oscillator (4.11). We take  $N = 100$ . For each  $E$ , we fix  $E^{(2)}$  through the relation shown in Fig. 11 and use it as the input parameter in the bootstrap analysis (4.14). We observe that the bootstrap method reproduces the numerical prediction (the dashed line) as  $(K_x, K_p)$  increase. Particularly, at  $K_x = K_p = 7$ , the results of the bootstrap method are almost coincident with the numerical ones. However, the bootstrap method does not work properly in higher energy region  $E/N > 0.65$ .

cannot be evaluated through the bootstrap method.

One possibility to obtain temperature is to introduce a “thermometer”. We prepare a system whose spectrum is well known, for example, harmonic oscillator, as a thermometer, and turn on weak interactions between this system and the target system, which we want to investigate. Then, from the spectrum of the thermometer system, we might be able to read the temperature of the entire system, and we might obtain the temperature dependence of the target system. However, it is unclear whether the bootstrap method works in such a interacting system, and we leave this as a future problem.

## 5 Discussions

We have presented that the bootstrap method can be used to obtain the bounds of possible expectation values of various physical quantities of the system under the constraint  $E = \langle H \rangle$ . Since the numerical bootstrap method can be regarded as a generalization of the uncertainty relation, the bounds of such physical quantities may be determined as a consequence of these uncertainty relations. We have also seen that the bounds of the possible values are further restricted through the additional constraints  $\langle [H, O] \rangle = 0$  for the stationary states (2.24) and  $\langle [H, O] \rangle = 0$  and  $\langle HO \rangle = E \langle O \rangle$  for the energy eigenstates (2.26). In this way, the difference between these three states in quantum mechanics is described by the difference of the constraints on expectation values in the bootstrap method.

These properties may reveal novel aspects of quantum mechanics. Particularly, our results indicate that the energy eigenstates may be determined through the uncertainty relations in a broad sense. It may be valuable to pursue this question and understand these algebraic structures of quantum mechanics further.

On the other hand, we found that there are no suitable constraints that describe the difference between the identical bosons and fermions. It is also difficult to describe the thermal equilibrium states in canonical ensemble because there are no useful constraints which specify the temperatures. These difficulties may be a sort of no go theorems, and it may be valuable to investigate these issues further. There might be some profound reasons why the bootstrap method does not work in these situations.

Another interesting direction is considering the bootstrap problem in lattice models and quantum field theories [7, 25, 26, 27, 28, 29]. Especially, the issue of the identical particles might be evaded in the second quantized picture, where they are described by a single quantum field. We leave this as a future problem.

**Acknowledgements** The author would like to thank Takehiro Azuma, Masafumi Fukuma, Koji Hashimoto, Satoru Odake, Junji Suzuki and Asato Tsuchiya for valuable discussions and comments. The author would also like to thank Yu Nakayama for valuable discussions and pointing out some issues in my numerical analysis on the YMQM. The author is especially grateful to Yu Aikawa and Kota Yoshimura for very helpful correspondence and collaboration at an early stage of this project. The author would like to thank participants of the YITP workshop “Strings and Fields 2021” (YITP-W-21-04, 23 August to 27 August 2021), “Strings and Fields 2022” (YITP-W-22-09, 19 August to 23 August 2022) and “Thermal Quantum Field Theory and Their Applications 2021” (KEK, 30 August to 1 September 2021) for stimulating discussions where part of this work was presented. A part of numerical computation in this work was carried out at the Yukawa Institute Computer Facility. The work of T. M. is supported in part by Grant-in-Aid for Scientific Research C (No. 20K03946) from JSPS.

## A Analytic Results on the Bounds

In this appendix, we explain details of some analytical results on the problems of the expectation values of physical quantities.

### A.1 States saturating the bound (2.4)

We derive the states that saturate the inequality (2.4) in the harmonic oscillator (2.2). This inequality is saturated when all the inequalities of (2.3) are saturated. Therefore  $\Delta x^2 = \Delta p^2 = \hbar/2$  must be satisfied. This is the relation satisfied by coherent states. From this, we find the states  $\exp(\mp ipx_*(E)/\hbar)|0\rangle$ , where  $|0\rangle$  is the ground state of the harmonic oscillator and  $x_*(E)$  is defined in (2.4). (This state is derived from the ground state  $|0\rangle$  translated by  $\pm x_*(E)$ .) Actually, we can easily show that these states satisfy  $E = \langle H \rangle$  and saturate the bounds (2.4) as,

$$\langle 0|e^{ipx_*/\hbar}He^{-ipx_*/\hbar}|0\rangle = \langle 0|H|0\rangle + \frac{1}{2}(x_*(E))^2 = E, \quad \langle 0|e^{ipx_*/\hbar}xe^{-ipx_*/\hbar}|0\rangle = x_*(E). \quad (\text{A.1})$$

Here we have used  $\langle 0|x|0\rangle = 0$  and  $\langle 0|H|0\rangle = \hbar/2$ .

### A.2 States saturating the bound (2.5)

We derive the states that saturate the inequality (2.5) in the harmonic oscillator (2.2). This inequality is saturated when  $\langle x^2 \rangle \langle p^2 \rangle = \hbar^2/4$  is satisfied, and we know that gaussian wave packets with  $\langle x \rangle = \langle p \rangle = 0$  satisfy it. Indeed, if we take the deviation of the gaussian wave packets as

$$\langle x^2 \rangle = E + \sqrt{E^2 - \hbar^2/4}, \quad (\text{A.2})$$

$\langle x^2 \rangle$  saturates the upper bound of (2.5). Then this gaussian wave packet satisfies  $\langle p^2 \rangle = E - \sqrt{E^2 - \hbar^2/4}$ , and we obtain  $\langle H \rangle = E$ . Similarly, if we take  $\langle x^2 \rangle = E - \sqrt{E^2 - \hbar^2/4}$ , it saturates the lower bound.

Note that the coherent states discussed in Appendix A.1 and the gaussian wave packets are the most fundamental states in quantum mechanics. It is an interesting conclusion that these states have the properties of maximizing (minimizing)  $\langle x \rangle$  and  $\langle x^2 \rangle$  in the harmonic oscillator.

### A.3 Bounds on $\langle p \rangle$ in general $V(x)$

We derive the upper and lower bounds on  $\langle p \rangle$  for general non-relativistic quantum mechanical systems,

$$H = \frac{1}{2}p^2 + V(x). \quad (\text{A.3})$$

We will show that the answer is given as

$$-p_* \leq \langle p \rangle \leq p_*, \quad p_*(E) := \sqrt{2(E - E_0)}, \quad (\text{A.4})$$

where  $E_0$  is the energy of the ground state. We prove it by contradiction. Suppose a state  $|\alpha\rangle$  satisfies  $E = \langle\alpha|H|\alpha\rangle$  and  $\tilde{p} = \langle\alpha|p|\alpha\rangle$ , where  $\tilde{p} > p_*(E)$  and violates the bound (A.4). Then we can define the state  $e^{-i\tilde{p}x/\hbar}|\alpha\rangle$ , and it satisfies

$$\langle\alpha|e^{i\tilde{p}x/\hbar}He^{-i\tilde{p}x/\hbar}|\alpha\rangle = \langle\alpha|H|\alpha\rangle + \frac{1}{2}\tilde{p}^2 - \tilde{p}\langle\alpha|p|\alpha\rangle = E - \frac{1}{2}\tilde{p}^2 < E_0. \quad (\text{A.5})$$

Thus, the energy is lower than the ground state, and the state  $|\alpha\rangle$  is inconsistent. Hence, there is no state which satisfies  $\tilde{p} > p_*(E)$  and the bound (A.4) is proved.

Besides, we can easily show that the state  $e^{\pm ip_*x/\hbar}|0\rangle$  saturates the inequalities in (A.4), where  $|0\rangle$  is the ground state. The proof is similar to (A.1) but we need to use  $\langle 0|p|0\rangle = 0$ , which can be shown by using the relation (2.23) with  $O = x$ .

The result (A.4) indicates that  $E - E_0$  yields the maximum value of  $|\langle p\rangle|$ . This may be reasonable, since  $|\langle p\rangle| > 0$  always causes an excitation from the ground state.

Note that  $p$  is quadratic in the Hamiltonian (A.3), and it is crucial in the above derivation of the bounds. Therefore, it seems difficult to apply this method to obtain the bounds on  $\langle x\rangle$  in (A.3).

#### A.4 Bounds on $\langle x_1\rangle$ in two non-interacting harmonic oscillators

We show the derivation of the bounds (3.4), (3.5) and (3.6) on  $\langle x_1\rangle$  in the two non-interacting harmonic oscillators,

$$H = \sum_{i=1}^2 \frac{1}{2}p_i^2 + \frac{1}{2}x_i^2. \quad (\text{A.6})$$

Since  $x_1$  is quadratic in this Hamiltonian, we can apply the method used in Appendix A.3.

The ground states and the ground energies of this system is given by

$$\text{Two distinct particles: } |0\rangle_2 := |0, 0\rangle, \quad E_0 = \hbar, \quad (\text{A.7})$$

$$\text{Two identical bose particles: } |0\rangle_B := |0, 0\rangle, \quad E_0 = \hbar, \quad (\text{A.8})$$

$$\text{Two identical fermi particles: } |0\rangle_F := \frac{1}{\sqrt{2}}(|1, 0\rangle - |0, 1\rangle), \quad E_0 = 2\hbar, \quad (\text{A.9})$$

where  $|m, n\rangle := (a_1^\dagger)^m(a_2^\dagger)^n|0, 0\rangle$ . Then, by translating these ground states by  $U(x_*) := e^{-ip_1x_*}$ , we may obtain the states which provide the maximum value of  $|\langle x_1\rangle|$  as in Appendix A.3. However, this translation operator is not symmetric under the particle exchange. Hence, it cannot be used for the identical particles, and we modify it as  $e^{-i(p_1+p_2)x_*}$ . Here  $x_*$  should be determined to satisfy

$E = \langle 0|U(x_*)^\dagger H U(x_*)|0\rangle$  for each ground state, and we obtain

$$\text{Two distinct particles: } E = \langle 0|H|0\rangle_2 + \frac{1}{2}x_*^2 \Rightarrow x_*^2 = 2(E - \hbar), \quad (\text{A.10})$$

$$\text{Two identical bose particles: } E = \langle 0|H|0\rangle_B + x_*^2 \Rightarrow x_*^2 = E - \hbar, \quad (\text{A.11})$$

$$\text{Two identical fermi particles: } E = \langle 0|H|0\rangle_F + x_*^2 \Rightarrow x_*^2 = E - 2\hbar. \quad (\text{A.12})$$

Similar to the proof in Appendix A.3, we can show that, if  $|\langle x_1 \rangle|$  exceeds  $x_*$ , it causes a contradiction and such a state is not allowed. Thus,  $x_*$  provides the maximum bound.

## References

- [1] Xizhi Han, Sean A. Hartnoll, and Jorrit Kruthoff. Bootstrapping Matrix Quantum Mechanics. *Phys. Rev. Lett.*, 125(4):041601, 2020.
- [2] Marcos Rigol, Vanja Dunjko, Vladimir Yurovsky, and Maxim Olshanii. Relaxation in a completely integrable many-body quantum system: An ab initio study of the dynamics of the highly excited states of 1d lattice hard-core bosons. *Phys. Rev. Lett.*, 98:050405, Feb 2007.
- [3] Thomas Curtright and Cosmas K. Zachos. Negative probability and uncertainty relations. *Mod. Phys. Lett. A*, 16:2381–2385, 2001.
- [4] Jun John Sakurai and Jim Napolitano. *Modern Quantum Mechanics*. Quantum physics, quantum information and quantum computation. Cambridge University Press, 10 2020.
- [5] Yu Nakayama. Bootstrapping microcanonical ensemble in classical system. *Mod. Phys. Lett. A*, 37(09):2250054, 2022.
- [6] David Berenstein and George Hulsey. Anomalous Bootstrap on the half line. 6 2022.
- [7] Scott Lawrence. Bootstrapping Lattice Vacua. 11 2021.
- [8] Yu Aikawa, Takeshi Morita, and Kota Yoshimura. Bootstrap Method in Harmonic Oscillator. *Physics Letters B*, 833:137305, 2022.
- [9] David Berenstein and George Hulsey. Bootstrapping Simple QM Systems. 8 2021.
- [10] Jyotirmoy Bhattacharya, Diptarka Das, Sayan Kumar Das, Ankit Kumar Jha, and Moulindu Kundu. Numerical bootstrap in quantum mechanics. *Phys. Lett. B*, 823:136785, 2021.
- [11] Xihe Hu. Different Bootstrap Matrices in Many QM Systems. 5 2022.
- [12] Yu Aikawa, Takeshi Morita, and Kota Yoshimura. Application of bootstrap to a  $\theta$  term. *Phys. Rev. D*, 105(8):085017, 2022.
- [13] David Berenstein and George Hulsey. Bootstrapping More QM Systems. 9 2021.
- [14] Serguei Tchoumakov and Serge Florens. Bootstrapping Bloch bands. *J. Phys. A*, 55(1):015203, 2022.
- [15] Bao-ning Du, Min-xin Huang, and Pei-xuan Zeng. Bootstrapping Calabi-Yau Quantum Mechanics. 11 2021.

- [16] Dong Bai. Bootstrapping the deuteron. 1 2022.
- [17] Wenliang Li. The null bootstrap. 2 2022.
- [18] Sakil Khan, Yuv Agarwal, Devjyoti Tripathy, and Sachin Jain. Bootstrapping PT symmetric Hamiltonians. 2 2022.
- [19] Sergei G. Matinyan, G. K. Savvidy, and N. G. Ter-Arutunian Savvidy. CLASSICAL YANG-MILLS MECHANICS. NONLINEAR COLOR OSCILLATIONS. *Sov. Phys. JETP*, 53:421–425, 1981.
- [20] G. K. Savvidy. Classical and Quantum Mechanics of Nonabelian Gauge Fields. *Nucl. Phys. B*, 246:302–334, 1984.
- [21] Tetsuya Akutagawa, Koji Hashimoto, Toshiaki Sasaki, and Ryota Watanabe. Out-of-time-order correlator in coupled harmonic oscillators. *JHEP*, 08:013, 2020.
- [22] Barry Simon. Some quantum operators with discrete spectrum but classically continuous spectrum. *Annals of Physics*, 146(1):209–220, 1983.
- [23] Anatoli Polkovnikov, Krishnendu Sengupta, Alessandro Silva, and Mukund Vengalattore. Nonequilibrium dynamics of closed interacting quantum systems. *Rev. Mod. Phys.*, 83:863, 2011.
- [24] Luca D’Alessio, Yariv Kafri, Anatoli Polkovnikov, and Marcos Rigol. From quantum chaos and eigenstate thermalization to statistical mechanics and thermodynamics. *Adv. Phys.*, 65(3):239–362, 2016.
- [25] Peter D. Anderson and Martin Kruczenski. Loop Equations and bootstrap methods in the lattice. *Nucl. Phys. B*, 921:702–726, 2017.
- [26] Henry W. Lin. Bootstraps to strings: solving random matrix models with positivite. *JHEP*, 06:090, 2020.
- [27] Vladimir Kazakov and Zechuan Zheng. Analytic and numerical bootstrap for one-matrix model and “unsolvable” two-matrix model. *JHEP*, 06:030, 2022.
- [28] Vladimir Kazakov and Zechuan Zheng. Bootstrap for Lattice Yang-Mills theory. 3 2022.
- [29] Minjae Cho, Barak Gabai, Ying-Hsuan Lin, Victor A. Rodriguez, Joshua Sandor, and Xi Yin. Bootstrapping the Ising Model on the Lattice. 6 2022.